



Energy, Mines and
Resources Canada

Énergie, Mines et
Ressources Canada

CANMET

Canada Centre for
Mineral and Energy
Technology

Centre canadien de la
technologie des
minéraux et de l'énergie

**Mining
Research
Laboratories**

**Laboratoires
de recherche
minière**

BIAXIAL TESTS OF SOME OVERCORED SAMPLES
FROM AECL'S UNDERGROUND RESEARCH
LABORATORY, LAC DU BONNET, MANITOBA

J.S.O. Lau
Mining Research Laboratories
Divisional Report MRL 89-55(TR)

1-7987296 c.2

May 1989

CPUB

c.2

**Declassified
Déclassifié**

2020-07-28

Canada

This document was produced
by scanning the original publication.

This document was produced
by scanning the original publication.

MRL 89-55 (TR) c.2

MRL 89-55 (TR) c.2

Canmet Information
Centre
D'information de Canmet

JAN 30 1997

555, rue Booth ST.
Ottawa, Ontario K1A 0G1

1-7987296 c.2

CPUB

BIAXIAL TESTS OF SOME OVERCORED SAMPLES
FROM AECL'S UNDERGROUND RESEARCH
LABORATORY, LAC DU BONNET, MANITOBA

1-7987296 c.2

J.S.O. Lau

May 1989

Mining Research Laboratories

CPUB

Divisional Report MRL 89-55(TR)

c.2

CANMET LIBRARY



3 2329 00061408 6

c.2

CPUB

BIAXIAL TESTS OF SOME OVERCORED SAMPLES FROM AECL'S
UNDERGROUND RESEARCH LABORATORY, LAC DU BONNET, MANITOBA

by

J.S.O. Lau¹

ABSTRACT

In support of Atomic Energy of Canada Limited's in situ stress measurement program at the Underground Research Laboratory, biaxial tests and biaxial tests with axial load were conducted at the Canada Centre for Mineral and Energy Technology (CANMET) to examine the effect of axial and side loads on the strains measured on the inside and on the outside of overcored rock samples obtained in the URL and the elastic constants derived from them. The rock is a massive, grey, medium to coarse grained porphyritic granite.

With axial loading, cell pressures as high as 36 MPa could be applied on the overcored specimens without causing disk ing. Without axial loading, a cell pressure as low as 13 MPa could cause disk ing.

There were fairly good agreements between the secant Young's modulus values obtained on the outside and on the inside of the hollow rock specimens in both the biaxial tests and the biaxial tests with axial load.

The secant Young's modulus values in the axial direction were found to be approximately 10 GPa higher than the modulus values in the circumferential direction, indicating that the rock specimens were highly anisotropic and the anisotropy was probably caused by the microcracks present in the specimens.

The secant Young's modulus values obtained in the biaxial tests with axial load at pressure levels above 28 MPa were very high. Selected uniaxial compression tests should be conducted on the overcored specimens to check the effect of end constraint on the modulus values as well as to shed some light on the discrepancies in some of the axial strain readings.

¹Geotechnical Engineer, Atomic Energy of Canada Limited, on attachment to Canadian Mine Technology Laboratories, Mining Research Laboratories, CANMET, Energy, Mines and Resources Canada, Ottawa, Ontario.

Keywords: overcore, biaxial, axial load, cell pressure, stress, strain, Young's modulus, Poisson's ratio, microcracks, anisotropy

**ESSAIS BIAXIAUX DE QUELQUES ÉCHANTILLONS SURCAROTTÉS
PROVENANT DU LABORATOIRE DE RECHERCHE SOUTERRAIN
DE L'EACL, LAC DU BONNET, MANITOBA**

par

J.S.O. Lau¹

RÉSUMÉ

Un programme de mesure de contraintes *in situ* a été mis en oeuvre par L'Énergie atomique du Canada Limitée (EACL) à son Laboratoire de recherche souterrain. Pour compléter ce programme, les chercheurs du Centre de la technologie des minéraux et de l'énergie (CANMET), ont mené des essais biaxiaux et des essais biaxiaux avec charge axiale pour étudier les effets des charges axiales et latérales sur les contraintes mesurées à l'intérieur et à l'extérieur des échantillons de roche surcarottés obtenus au LRS de même que sur les constantes élastiques qui en résultent. La roche est massive, grise et composée de granit pophyritique à moyens et à gros grains.

Quand la charge axiale est appliquée, des chambres de pression équivalant 36 MPa peuvent être appliquées sur les échantillons surcarottés sans causer de rupture. Sans la charge axiale, une chambre de pression aussi faible que 13 MPa peut être la cause d'une rupture.

Les valeurs de la sécante établies par le module de Young à l'extérieur et à l'intérieur des échantillons de roche creux étaient semblables à celles obtenues, à la fois dans les essais biaxiaux et les essais biaxiaux avec charge axiale.

Les valeurs de la sécante dérivées du module de Young en direction axiale étaient approximativement de 10 GPa plus grandes que celles en direction circonférentielle. Ce fait indique que l'anisotropie très élevée des échantillons de roche était probablement causée par des micro-fissures dans les échantillons.

Les valeurs de la sécante établies par le module de Young dans les essais biaxiaux avec charge axiale à des taux de pression supérieurs à 28 MPa étaient très élevées. Des

¹Ingénieur géotechnique, Énergie atomique de Canada Limitée, détaché aux Laboratoires canadiens de technologie minière, Laboratoires de recherche minière, CANMET, Énergie, Mines et Ressources Canada, Ottawa, Ontario.

essais de compression uniaxiale sélectionnés devraient être menés sur les échantillons surcarottés pour vérifier l'effet de la contrainte latérale sur les valeurs du module de même que pour mettre en lumière les divergences qui se manifestent dans certains relevés de contraintes axiales.

Mots-clé: surcarottage, biaxiale, charge biaxiale, chambre de pression, contrainte, module de Young, déformation, coefficient de Poisson, micro-fissures, anisotropie.

CONTENTS

	<u>Page No.</u>
ABSTRACT	i
RÉSUMÉ	ii
1. INTRODUCTION	1
2. SAMPLING AND SPECIMEN PREPARATION	2
2.1 Sampling	2
2.2 Preparation of cylindrical rock specimens	2
2.3 Installation of the CSIR cell	2
2.4 Application of strain gauges	3
3. TEST APPARATUS AND PROCEDURE	3
3.1 Hoek triaxial cell	3
3.2 Biaxial tests	4
3.3 Biaxial tests with axial load	4
4. ANALYSIS OF STRESSES	5
4.1 Analysis of stresses in biaxial tests	5
4.2 Analysis of stresses in biaxial tests with axial load	7
5. RESULTS AND DISCUSSION	8
5.1 Test results	8
5.2 Strains	8
5.3 Modulus of elasticity	9
5.4 Poisson's ratio	11
6. CONCLUSIONS	11
7. RECOMMENDATIONS	12
ACKNOWLEDGEMENTS	13
REFERENCES	13
Appendix A. Specimen 208-019-OC1-10.72	35
Appendix B. Specimen 208-019-OC1-13.54	38
Appendix C. Specimen 208-019-OC1-14.55	47
Appendix D. Specimen 208-019-OC1-15.50	56

1. Introduction

Atomic Energy of Canada Limited (AECL) has constructed an Underground Research Laboratory (URL) in the Lac du Bonnet Batholith, located 100 km northeast of Winnipeg, Manitoba. The URL will be used to investigate some of the issues associated with the concept of the safe design, construction and operation of a vault for the disposal of high-level nuclear waste deep in plutonic rock. One of the issues is whether the in situ stress condition in a plutonic rock body and the stresses induced around an excavation in such a body can be understood. The stresses affect not only the stability of the excavation, but also the development of damaged zones around the excavation, which are potential pathways for radionuclide leakage from the vault.

A comprehensive in situ stress measurement program is underway at the URL (Simmons and Soonawala, 1982; Lang et al., 1986; Wright, 1988). Several stress measurement techniques are used, including methods which utilize the modified CSIR triaxial strain cell. The instrument makes use of three rosettes, each containing four strain gauges, which are glued on the borehole wall. The gauges measure strains resulting from overcoring which, in turn, can be used to determine in situ stresses according to equations derived from the theory of elasticity (Leeman, 1968; Van Heerden, 1973; Herget et al., 1978; Vreede, 1981).

Effective use of the CSIR triaxial strain cell for determining the in situ stresses depends on the accuracy of the estimates of the modulus of elasticity and Poisson's ratio of the rock at the measuring point. The modulus of elasticity and the Poisson's ratio are usually determined in the laboratory by carrying out standard uniaxial compression tests on EX core samples or by conducting biaxial tests on the overcore samples. In the uniaxial compression test, the elastic constants are calculated from strains measured by strain gauges on the outside of the core sample. However, in the biaxial test, the elastic constants are determined from strains measured by the CSIR cell on the inside of the hollow cylindrical overcore sample. A study was undertaken by Canada Centre for Mineral and Energy Technology (CANMET) and AECL to examine the effect of various combinations of axial and side loads on the strains measured on the inside and on the outside of the overcore samples and the elastic constants derived from them. The results are presented in this report. It is hoped that the results will provide some insight into the stress relief behaviour of the core during overcoring and subsequently the in situ stresses derived from it. It was also felt that the end constraint would enable the application of higher side loads (greater than 26 MPa) which were causing disking in the absence of axial loading.

2. Sampling and specimen preparation

2.1 Sampling

Specimens were prepared from 96-mm hollow overcored samples with EX pilot holes obtained from Borehole 208-019-OC1 in the Underground Research Laboratory at the 240-m level. The trend and plunge of the borehole are 051.04° and -27.23° respectively. The rock is a massive, grey, medium to coarse grained porphyritic granite, composed of quartz, K-feldspar, plagioclase and biotite. The mean horizontal stress at the 240-m level was reported to be 28.04 MPa (Lang et al., 1986).

2.2 Preparation of cylindrical rock specimens

Cylindrical test specimens were prepared in accordance to the procedure described in the Pit Slope Manual Supplement 3-5 (Gyenge and Ladanyi, 1977) and the method suggested by the International Society for Rock Mechanics (Brown, 1981). Specimens were first cut slightly larger than their final dimensions from the overcored samples by means of a water-cooled diamond saw in CANMET's Elliot Lake Laboratory and then the end surfaces of each specimen were ground to parallel within 0.05 mm to ensure that the end surfaces were parallel to each other and perpendicular to the axis of the specimen.

After the specimens had been prepared, they were sent back to CANMET's Mining Research Laboratories in Ottawa. The EX holes of the specimens were flushed with water, cleaned and dried. The outer and inner diameters and the length of each specimen were measured and the dimensions are shown in Table 1. The dimensions of the specimens varied from 86.38 to 86.39 mm in outer diameter, 37.73 to 37.96 mm in inner diameter and 351 to 352 mm in length, with length to outer diameter ratios ranging from 4.06 to 4.08.

2.3 Installation of the CSIR cell

The CSIR cells used in these tests are composed of three 120 ohm four-element rosettes with a gauge factor of 2.07 and a normal gauge excitation of 2 volts. Before the CSIR cell was installed, the cell was plugged into the front end of the installation tool and the strain gauges in the cell were tested one by one to make sure all gauges were in good working condition. To prepare the cell for installation, the three rosettes on the cell were first rubbed with emery paper to remove the shiny appearance of the

gauges and then cleaned with acetone. A glue was mixed and a 1 to 2 mm thick layer was applied to each rosette. Immediately after this, the assembly was pushed into the EX hole of the specimen. The CSIR cell was placed at approximately midheight of the specimen and oriented in such a way that pin B in the cell was aligned with the reference line on the core specimen. The rosette plugs in the CSIR cell were then forced out of the cell body by means of a pneumatically actuated rod which protruded from the front end of the installation tool. The cell was held in that position until the glue had set. Once the glue had set, the installation tool was removed, leaving the cell in the EX hole inside the specimen.

2.4 Application of strain gauges

Strain gauges were applied on the outside of each of the cylindrical specimens to determine the axial and circumferential strains on the outside of the specimen. The BLH Electronics, SR-4, FAE series strain gauges with a gauge factor of 2.01 and gauge length of 12.70 mm were used. Two diametrically opposed axial strain gauges were mounted at midheight of the specimen. Two circumferential strain gauges were similarly mounted at 90° to the axial gauges. In each case, the two gauges were connected in series to form a single active gauge. Very thin ribbon leads were used to ensure that the specimen could fit into the rubber jacket in the Hoek Triaxial cell (see Section 3.1). The ribbon leads were waterproofed by coating with BLH Barrier B. It should be noted that the resistance of the ribbon lead is very high and its use as leads should be restricted to those sections to be inserted into the rubber jacket. Outside the rubber jacket, low resistance insulated wires were used for leads.

3. Test apparatus and procedure

3.1 Hoek triaxial cell

The biaxial chamber used to conduct these tests was the Hoek triaxial cell comprised of a steel body, two steel end caps and two self-sealing couplings, one for connecting to the hydraulic pressure system and the other for de-airing and draining the cell chamber. The cell chamber measures approximately 10.80 cm in diameter and 34.93 cm in length and is fitted with a rubber jacket. Details about the Hoek triaxial cell and its assembly can be found in various papers (Hoek and Franklin, 1968; Franklin and Hoek, 1970) and therefore will not be repeated in this report. An exception to the standard procedure is that the specimen was inserted into the rubber jacket before the

insertion of the jacket into the cell chamber. Experience has shown that by using this procedure, the risks of breaking the leads and overstressing the strain gauges mounted on the outside of the specimen are greatly reduced.

3.2 Biaxial tests

To set up the apparatus for the biaxial test, a cable with a cable head was first pushed into the EX hole of the hollow cylindrical specimen so as to connect the CSIR cell to a switch box. The switch box was then connected in a three wire quarter-bridge configuration to a B & K ZR 0014 quarter-bridge adaptor plugged into a B & K type 1526 strain indicator for strain measurements. The strain gauges mounted on the outside of the specimen were connected in a half-bridge configuration to another B & K strain indicator. The assembling of the apparatus was completed by filling up the Hoek cell chamber with oil.

In the biaxial test, each specimen was subjected to three cycles of loading and unloading. A maximum biaxial cell pressure of only 10 MPa was applied because specimen disking occurred at the cell pressure of approximately 13 MPa in the first trial test. In each cycle, the biaxial cell pressure was raised from 0 to 10 MPa and then lowered from 10 to 0 MPa in intervals of 1 MPa. At each interval, the strain readings of all 12 strain gauges of the CSIR cell and the strain gauges mounted on the outside of the specimen were taken.

After the biaxial test had been completed, the oil in the Hoek biaxial cell was drained and the installation tool was disconnected from the CSIR cell. The specimen and the rubber jacket were then simultaneously removed from the Hoek cell chamber. No attempt was made to remove the specimen from the rubber jacket to allow for subsequent testing with axial load.

3.3 Biaxial tests with axial load

The Hoek cell was set up in a MTS 815 rock mechanics test system for the biaxial test with axial load. The MTS system is a servo-hydraulic press consisting of a load frame, load cell, hydraulic power supply, confining pressure subsystem, test controller, test processor and DEC micro PDP 11/73 computer. For a detailed description of the MTS system and its operation, the reader is referred to the MTS operation manual (MTS Systems Corp., 1986). To set up the axial loading system, a platen was placed on top of the specimen and the ram was extended until it touched the top platen. The top platen is hollow and measures 225.7 mm in length, 86.0 mm in outside diameter

and 37.8 mm in inside diameter and has a 19.8 mm diameter hole at the side to allow the passage of the cable connecting the CSIR cell to the switch box. The leads from the strain gauges and the cable from the CSIR cell were connected to the strain indicators as described in Section 3.2 for strain measurements. Finally, the Hoek cell was connected to the MTS confining pressure subsystem. A small axial load was applied and the Hoek cell chamber was filled with Syltherm 800 heat transfer liquid.

Each specimen was again subjected to three cycles of loading and unloading. The axial pressure and the cell pressure were raised simultaneously in intervals of 2 MPa from 0 MPa to the maximum pressure of 36 MPa and then lowered back to 0 MPa in the same manner. A maximum pressure of 36 MPa was applied to coincide with the maximum horizontal stress of 32.33 MPa reported by Lang et al. (1986) at the URL. The operation was computer-controlled. The axial loading was regulated by the test controller and the cell pressure was generated by the confining pressure subsystem according to the commands given by the operator. At each interval, the strain readings of all 12 strain gauges of the CSIR cell and the strain gauges mounted on the outside of the specimen were taken.

After the test had been completed, the liquid was drained from the cell chamber. The Hoek triaxial cell was then removed from the MTS system, and the specimen and the jacket were removed from the cell chamber as described in Section 3.2.

4. Analysis of stresses

In these tests, the hollow cylindrical specimens can be treated as thick-walled cylinders subjected to an external pressure and therefore, equations previously developed by Seely and Smith (1967) for the analysis of stresses in a hollow cylinder under an external pressure and an internal pressure can be used to analyse the results obtained from these tests.

4.1 Analysis of stresses in biaxial tests

In the biaxial test, the specimen can be treated as an open-ended thick-walled cylinder. The circumferential stress σ_t at a point at any distance ρ from the central axis of a relatively long open-ended thick-walled cylinder is given as follows:

$$\sigma_t = -\frac{p_1 r_1^2 - p_2 r_2^2 + (r_1^2 r_2^2 / \rho^2)(p_1 - p_2)}{r_2^2 - r_1^2} \quad (1)$$

where r_1 = inside radius of the cylinder
 r_2 = outside radius of the cylinder
 p_1 = internal pressure
 p_2 = external pressure

If the internal pressure is zero ($p_1 = 0$), as in the biaxial test, Eq. 1 reduces to:

$$\sigma_t = p_2 \frac{r_2^2}{r_2^2 - r_1^2} \left(1 + \frac{r_1^2}{\rho^2}\right) \quad (2)$$

The circumferential stress σ_t is compressive. At the inner surface (when $\rho = r_1$), that is, on the inside of the specimen, σ_t has its maximum value and is found to be:

$$\sigma_t = 2p_2 \left(\frac{r_2^2}{r_2^2 - r_1^2}\right) \quad (3)$$

At the outer surface (when $\rho = r_2$), that is, on the outside of the specimen, σ_t has its minimum value and is:

$$\sigma_t = p_2 \left(\frac{r_2^2 + r_1^2}{r_2^2 - r_1^2}\right) \quad (4)$$

Since σ_t is related to the circumferential strain e_t by the Young's modulus E_t (circumferential), the substitution of $\sigma_t = E_t e_t$ into Eqs. 3 and 4 gives the following equations for the determination of the Young's modulus:

$$E_t = \frac{2p_2}{e_t} \left(\frac{r_2^2}{r_2^2 - r_1^2}\right) \quad (5)$$

where e_t is one of the three circumferential strains, e_3 , e_7 and e_{11} , measured by the CSIR cell on the inside of the specimen, and

$$E_t = \frac{p_2}{e_t} \left(\frac{r_2^2 + r_1^2}{r_2^2 - r_1^2}\right) \quad (6)$$

where e_t is the circumferential strain measured by the strain gauges on the outside of the specimen.

The Poisson's ratio is expressed in the biaxial test as the ratio of the axial strain, e_l , to the circumferential strain, e_t , and can be written as:

$$\nu = \frac{e_l}{e_t} = \frac{e_1}{e_3} = \frac{e_5}{e_7} = \frac{e_9}{e_{11}} \quad (7)$$

where e_1 , e_5 and e_9 are the axial strains measured by the CSIR cell.

4.2 Analysis of stresses in biaxial tests with axial load

In the biaxial test with axial load, the specimen can be treated as a closed-ended thick-walled cylinder. If the cylinder is subjected to an internal pressure p_1 and an external pressure p_2 which also act on the capped ends, the axial stress σ_l on any traverse section which is not close to the ends of the cylinder is found to be:

$$\sigma_l = -\frac{p_1 r_1^2 - p_2 r_2^2}{r_2^2 - r_1^2} \quad (8)$$

If the internal pressure is zero ($p_1 = 0$), as in the biaxial test with axial load, Eq. 8 reduces to:

$$\sigma_l = p_2 \left(\frac{r_2^2}{r_2^2 - r_1^2} \right) \quad (9)$$

The axial stress σ_l can also be related to the axial strain e_l by the Young's modulus E_l (axial). By substituting the value of $\sigma_l = E_l e_l$ into Eq. 9, the following equation is obtained:

$$E_l = \frac{p_2}{e_l} \left(\frac{r_2^2}{r_2^2 - r_1^2} \right) \quad (10)$$

Assuming an uniform distribution of σ_l on any traverse section which is not close to the ends of the specimen, e_l is the axial strain measured by the strain gauges on the outside of the specimen or one of the axial strains, e_1 , e_5 and e_9 , measured by the CSIR cell on the inside of the specimen.

5. Results and discussion

5.1 Test results

Four specimens (see Table 1) were tested at CANMET's Mining Research Laboratories in Ottawa. The biaxial tests were conducted first, followed by the biaxial tests with axial load. During each test, the specimen was subjected to three cycles of loading and unloading and the strain readings from the strain gauges and the CSIR cell were recorded. Equations 5, 6, 7 and 10 were used to calculate the values of secant Young's modulus and Poisson's ratio. Appendices A, B, C and D present the axial and circumferential strains measured and the values of secant Young's modulus and Poisson's ratio computed in each cycle of loading and unloading. Note that no meaningful data could be obtained from the CSIR cell installed in Specimen 208-019-OC1-10.72 probably due to the poor bonding of the cell to the rock, and therefore, those data were excluded from the results.

The unloading part of the third cycle of each of these tests produced the most satisfactory results and will be discussed in this report. The unloading curves (pressure vs. strain) are illustrated in Figures 1 to 8. Note that Figures 3 and 7 show that the CSIR axial strain gauge used to measure e_9 in Specimen 208-019-OC1-14.55 was not bonded properly to the rock, and therefore, e_9 would not be used in the analysis of the results from that specimen.

5.2 Strains

The plots of the external pressure versus circumferential strain for the biaxial tests (Figs. 1 to 4) indicate that the circumferential strains measured on the inside of the hollow specimens were greater than those measured on the outside of the specimens. This agrees very well with the theory which states that the maximum circumferential stress in a thick-walled cylinder occurs at its inner surface.

In the biaxial tests, the circumferential strains exhibited non-linear relationships, but the axial strains showed only slight non-linearity. This indicated the presence of

microcracks in the rock specimens and that the microcracks were subparallel to the axes of the specimens. The orientation of the microcracks on the 240-m level at the URL was reported to trend 020° to 040° (Martin, in prep.) and these specimens trends 051° . There is a good agreement between the orientation of the microcracks observed in these tests and that measured in the field.

The axial strains measured on the inside of the specimens in the biaxial tests were found to be smaller than those measured on the outside of the specimens (Figs. 1 to 4). A rational assumption concerning the strains in the thick-walled cylinder is that the axial strains on any traverse section which is not close to the ends of the cylinder are equal. One possible explanation for this discrepancy is that the gauge length of the CSIR cell is small in comparison with the grain size of the rock. At low strain levels, the CSIR cell might have measured the change in lengths of individual grains instead of the length of the overall specimen. It should also be noted that the effect of the cell pressure on the outside strain gauges is not known. More tests have to be carried out to investigate this discrepancy.

In the biaxial tests with axial load, the axial strains measured on the outside of the specimens agreed reasonably well with those measured on the inside of the specimens, as illustrated in Figures 5 to 8. The axial strains exhibited non-linearity because of possible crack closure. Full range uniaxial compression tests should be conducted on these overcored specimens to shed some light on this phenomenon.

5.3 Modulus of elasticity

The values of secant Young's modulus obtained from the strain measurements on the outside (strain gauges) and on the inside (CSIR cell) of each specimen at each test interval and their mean values are presented in Tables 2 and 3. Note that each modulus value on the inside is the average of the three values obtained from the three rosettes on the CSIR cell. The means of all modulus values (inside and outside) at each test interval and their standard deviations are also presented in Tables 2 and 3.

In Figures 9 to 12, the values of secant Young's modulus for each of the specimens were plotted against the external pressure. Biaxial test results are represented by dash dotted lines (outside values) and dotted lines (inside values). Results from the biaxial tests with axial load are represented by dash lines (outside values) and solid lines (inside values). From these plots, it can be seen that in two of the biaxial tests with axial load (Specimens 208-019-OC1-14.55 and 208-019-OC1-15.50), there was good agreement between the values of secant Young's modulus obtained on the inside and on the outside

of the specimens. However, in one test (Specimen 208-019-OC1-13.54), the modulus value on the inside was about 10 % higher than that on the outside. In the biaxial tests without end constraint, some discrepancies were found between the modulus values obtained on the outside and on the inside of the specimens.

The modulus-pressure curves for the outside and inside of all four specimens were plotted together in Figure 13 for the biaxial tests and in Figure 14 for the biaxial tests with axial load. Their mean values were plotted in Figures 15 and 16 respectively. In these figures, the solid lines represent the modulus values on the outside and the dash lines represent those on the inside of the specimens. Figure 15 shows that in the biaxial tests, the mean modulus values agreed fairly well with each other at the external pressure levels of 8 to 10 MPa. At the pressure levels of 1 to 7 MPa, the mean modulus values on the inside were higher (up to 10 %) than those on the outside. In the biaxial tests with axial load, although the mean modulus values on the inside were a little higher (2 to 6 %) than those on the outside, the pair of mean modulus curves compared fairly well with each other.

The modulus values determined in the biaxial tests with axial load were found to be approximately 10 GPa higher than those determined in the biaxial tests. The modulus values obtained in the biaxial tests with axial load were measured in the axial direction, but the modulus values obtained in the biaxial tests were measured in the circumferential direction. This indicates that the rock samples were highly anisotropic and the anisotropy was probably caused by the microcracks which were subparallel to the axes of the specimens.

The mean tangent Young's modulus values (axial) obtained in triaxial tests conducted by Lau et al. (1988) on the similar type of rock with similar orientation, at stress levels corresponding to 10% of the failure deviator stress, at the confining pressure levels of 3.5, 17.0 and 35.0 MPa were 54.35, 73.10 and 78.42 GPa respectively. The mean secant modulus values (circumferential) obtained in the biaxial tests were lower than those tangent modulus values (axial) as expected. However, the mean secant modulus values (axial) obtained in the biaxial tests with axial load were higher than those tangent modulus values (axial). The secant modulus values at pressure levels above 28 MPa were particularly high because of the complex axial loading conditions. Uniaxial compression with a focus on end friction effects should be performed on these overcored specimens to check the modulus values.

5.4 Poisson's ratio

The values of Poisson's ratio obtained in the biaxial tests were computed using Equation 7 and are given in Table 4. Note that the Poisson's ratio on the inside of each specimen at each pressure level is the average of the three values obtained from the three rosettes on the CSIR cell. The results show that the mean Poisson's ratio varied from 0.10 to 0.24 on the outside and from 0.02 to 0.07 on the inside of the specimens. The values obtained on the outside at pressure levels above 7 MPa agreed reasonably well with values obtained in other tests (Annor and Jackson, 1987). At pressure levels below 7 MPa, the values were lower, probably due to the closure of microcracks which were subparallel to the axes of the specimens. The Poisson's ratio values obtained on the inside were very low because the axial strains measured were very small. This problem has been discussed in Section 5.2.

6. Conclusions

The apparatus and procedures to carry out the biaxial test, and the biaxial test with axial load, and the equations to calculate the values of secant Young's modulus, and Poisson's ratio from the strain measurements have been developed and discussed in this report. In the biaxial tests with axial load, cell pressures as high as 36 MPa could be applied on the specimens without causing disking. With the absence of any axial load, a cell pressure as low as 13 MPa could cause disk. From the results of these tests, the following conclusions can be made.

(1) Biaxial tests:

The circumferential strains measured on the inside of the hollow specimens were greater than those measured on the outside of the specimens in agreement with the theory.

The circumferential strains exhibited non-linear relationships but the axial strains showed only slight non-linearity, indicating the presence of microcracks in the specimens and that the orientations of the microcracks were subparallel to the axes of the specimens.

Although some discrepancies were found between the secant Young's modulus values obtained on the outside and on the inside of the specimens in individual tests, their mean values compared fairly well (within 10 %) with each other.

The values of Poisson's ratio determined on the outside at pressure levels above 7 MPa agreed with, but those obtained at pressure levels below 7 MPa were lower than the values of Poisson's ratio obtained in other tests. No meaningful value of Poisson's ratio could be determined on the inside of the specimens because the axial strains measured were very small. Further testing is required to address this issue.

(2) Biaxial tests with axial load:

In the biaxial tests with axial load, the axial strains measured on the outside of the specimens agreed reasonably well with those measured on the inside.

With increased cell pressure, the incremental axial strains became less.

There were good agreements between the secant Young's modulus values obtained on the outside and on the inside of the specimens in two tests. The mean modulus values on the inside of all four specimens were found to be a little higher (2 to 6 %) than those on the outside.

(3) Anisotropy:

The secant Young's modulus values in the axial direction determined in the biaxial tests with axial load were approximately 10 GPa higher than the secant modulus values in the circumferential direction determined in the biaxial tests, indicating that the rock specimens were highly anisotropic and the anisotropy was probably caused by microcracks in the specimens.

7. Recommendations

The results of these tests show that the behaviour of the rock at the URL is anisotropic and non-linear. This behaviour must be taken into account in choosing the elastic constants for the calculation of rock stresses from strains measured during overcoring.

The axial strains measured in the biaxial test on the inside of the specimens were low and the secant Young's modulus values obtained in the biaxial tests with axial load seemed to be high. It is recommended that uniaxial compression tests be conducted on these specimens to check these values.

The biaxial test and the biaxial test with axial load are useful tests for checking the bonding of the CSIR cell to the rock as well as for investigating the anisotropy

of a rock specimen. It is recommended that these tests to be carried out on selected overcored samples with existing CSIR cells in any future URL overcoring program.

Acknowledgements

The author wishes to thank Dr. G. Herget and R. Jackson of CANMET for reviewing this report and making many helpful suggestions. Gratitude is expressed to B. Gorski of CANMET for setting up the apparatus for the biaxial tests with axial load in the MTS rock mechanics test system and writing the MTS basic program for the MTS automated system. The assistance of G. Murray in instrumenting the strain gauges is also appreciated.

References

- Annor, A. and Jackson, R. (1987), "Mechanical, thermomechanical and joint properties of rock samples from the Lac du Bonnet Batholith, Manitoba", in Geotechnical studies at Whiteshell Research Area (RA-3) (edited by Katsube, T.J. and Hume, J.P.), Division Report MRL 87-52(TR), CANMET, Energy, Mines and Resources Canada, 232 p.
- Brown, E.T. (1981), "Rock characterization testing and monitoring, ISRM suggested methods", International Society for Rock Mechanics, the Commission on Testing Methods, Pergamon, 211 p.
- Franklin, J.A. and Hoek, E. (1970), "Developments in triaxial testing technique", Rock Mechanics, Vol. 2, p. 223-228.
- Gyenge, M. and Ladanyi, B. (1977), "Pit slope manual supplement 3-5 - sampling and specimen preparation", CANMET, CANMET Report 77-29, 30 p.
- Herget, G., Miles, P. and Zawadski, W. (1978), "Equipment and procedures to determine ground stresses in a single drill hole", CANMET, CANMET Report 78-11, 22 p.
- Hoek, E. and Franklin, J.A. (1968), "A simple triaxial cell for field and laboratory testing of rock", Trans. Inst. Mining & Metallurgy, Vol. 77, p. A22-A26.
- Lang, P.A., Everitt, R.A., Ng, L.K.W. and Thompson, P.M. (1986), "Horizontal in situ stresses versus depth in the Canadian Shield at the underground research laboratory", in Proceedings of the International Symposium on Rock Stress and Rock Stress Measurements, Stockholm, September 1-3, 1986, p. 449-456.

Lau, J.S.O., Jackson, R. and Gorski, B. (1988), "High temperature triaxial tests on rock samples from boreholes 209-021-SV1 and 209-030-DIL1, Lac du Bonnet, Manitoba", Division Report MRL 88-112(TR), CANMET, Energy, Mines and Resources Canada, 57 p.

Leeman, E.R. (1968), "The determination of the complete state of stress in rock in a single borehole - laboratory and underground measurements", Int. J. Rock Mech. Min. Sci., Vol. 5, p. 31-56.

Martin, C.D. (in prep.), "Characterizing in situ stress domains at AECL's underground research laboratory", Proceedings of the 42nd Canadian Geotechnical Conference, Winnipeg, Manitoba, October 23-25, 1989.

MTS Systems Corporation (1986), "Operation manual for 815 rock mechanics test systems", MTS Systems Corp., Minneapolis, Minnesota, U.S.A.

Seely, F.B. and Smith, J.O. (1967), "Advanced Mechanics of Materials", John Wiley & Sons, 680 p.

Simmons, G.R. and Soonawala, N.M. (1982), "Underground research laboratory experimental program", Atomic Energy of Canada Limited Technical Record, TR-153, 126 p.

Van Heerden, W.L. (1973), "The influence of various factors on the triaxial strain cell results", CSIR Report ME 1178, 68 p.

Vreede, F.A. (1981), "Critical study of the method of calculating virgin rock stresses from measurement results of the CSIR triaxial strain cell", CSIR Report ME 1679, 62 p.

Wright, E.D. (1988), "Semi-annual status report of the Canadian Nuclear Fuel Waste Management Program, 1987 October 1 - 1988 March 31", Atomic Energy of Canada Limited Technical Record, TR-425-4, 201 p.

Table 1. Dimensions of specimens

Specimen identification	Outer diameter (mm)	Inner diameter (mm)	Cross-section area (cm ²)	Length (mm)	Length to outer diam. ratio
208-019-OC1-10.72	86.39	37.96	47.30	352	4.07
208-019-OC1-13.54	86.39	37.89	47.34	351	4.06
208-019-OC1-14.55	86.38	37.88	47.33	352	4.08
208-019-OC1-15.50	86.38	37.73	47.42	351	4.06

Table 2. Values of Young's modulus E_t obtained in the biaxial tests

Pressure (MPa)	Young's modulus on the outside						Young's modulus on the inside						Mean E_t (GPa)	Standard deviation (GPa)		
	E_t (GPa)				E_t (GPa)				E_t (GPa)							
	Specimens				Mean	s.d.	Specimens				Mean	s.d.				
	OC1- 10.72	OC1- 13.54	OC-1- 14.55	OC1- 15.50			OC1- 13.54	OC1- 14.55	OC1- 15.50							
10	49.28	44.34	33.55	33.83	40.25	7.84	34.03	49.52	37.13	40.23	8.20	40.24	7.29			
9	47.38	42.72	32.07	32.15	38.58	7.71	32.90	48.44	35.90	39.08	8.24	38.79	7.24			
8	45.57	40.31	30.41	30.58	36.72	7.50	31.56	46.49	34.43	37.49	7.92	37.05	7.02			
7	43.96	39.75	29.05	28.93	35.42	7.62	30.69	45.15	33.15	36.33	7.74	35.81	7.02			
6	41.45	36.60	27.55	27.42	33.26	6.95	29.13	43.72	31.91	34.92	7.75	33.97	6.70			
5	39.96	35.32	26.27	25.82	31.84	6.96	27.98	42.27	30.55	33.60	7.62	32.60	6.67			
4	37.89	34.14	24.43	24.32	30.20	6.89	27.21	41.19	29.35	32.58	7.53	31.22	6.65			
3	37.13	33.81	23.41	23.11	29.37	7.18	26.16	39.28	28.12	31.19	7.08	30.15	6.59			
2	34.55	32.09	22.05	22.30	27.75	6.51	25.24	38.63	27.76	30.54	7.12	28.95	6.35			
1	33.76	33.55	21.98	21.64	27.73	6.84	24.77	38.36	26.55	29.89	7.39	28.66	6.55			

Table 3. Values of Young's modulus E_l obtained in the biaxial tests with axial load

Pressure (MPa)	Young's modulus on the outside					Young's modulus on the inside					Mean E_l (GPa)	Standard deviation (GPa)		
	E_l (GPa)					E_l (GPa)								
	Specimens				s.d.	Specimens				s.d.				
	OC1- 13.54	OC1- 14.55	OC1- 15.50	Mean		OC1- 13.54	OC1- 14.55	OC1- 15.50	Mean					
36	81.79	98.39	100.20	93.46	10.15	90.08	97.57	98.43	95.36	4.59	94.41	7.12		
34	79.37	94.17	95.93	89.82	9.10	86.36	93.25	93.94	91.18	4.19	90.50	6.38		
32	76.94	90.66	92.39	86.66	8.46	82.64	90.90	91.33	88.29	4.90	87.48	6.25		
30	73.49	87.39	89.12	83.33	8.57	79.73	87.42	88.18	85.11	4.67	84.22	6.25		
28	70.04	83.74	85.44	79.74	8.44	76.81	84.59	85.07	82.16	4.64	80.95	6.23		
26	66.98	80.28	82.17	76.48	8.28	73.58	81.44	82.01	79.01	4.71	77.74	6.18		
24	63.91	76.78	78.88	73.19	8.11	70.34	78.37	78.84	75.85	4.78	74.52	6.13		
22	61.09	72.83	75.10	69.67	7.52	67.49	74.79	75.40	72.56	4.40	71.12	5.73		
20	58.27	69.17	71.43	66.29	7.04	64.64	71.42	72.36	69.47	4.21	67.88	5.47		
18	54.87	65.35	67.82	62.68	6.88	61.03	68.02	68.89	65.98	4.31	64.33	5.44		
16	51.46	61.52	64.20	59.06	6.72	57.42	64.51	66.22	62.72	4.67	60.89	5.55		
14	48.59	57.97	60.07	55.54	6.11	54.08	60.80	62.19	59.02	4.34	57.28	5.11		
12	45.72	54.22	56.82	52.25	5.81	50.73	56.97	58.68	55.46	4.18	53.86	4.85		
10	43.08	50.95	53.27	49.10	5.34	47.73	53.10	55.76	52.20	4.09	50.65	4.58		
8	40.43	48.08	49.93	46.15	5.04	44.72	48.89	52.14	48.58	3.72	47.37	4.18		
6	37.91	45.30	46.93	43.38	4.81	41.71	44.91	49.17	45.26	3.74	44.32	3.99		
4	35.38	44.22	44.53	41.38	5.20	38.69	40.93	46.61	42.08	4.08	41.73	4.20		
2		42.69	41.19				34.72	44.21			40.70	4.17		

Table 4. Values of Poisson's ratio ν obtained in the biaxial tests.

Pressure (MPa)	Poisson's ratio on the outside ν						Poisson's ratio on the inside ν					
	Specimens				Mean	Standard deviation	Specimens				Mean	Standard deviation
	OC1- 10.72	OC1- 13.54	OC-1 14.55	OC1- 15.50			OC1- 13.54	OC1- 14.55	OC1- 15.50			
10	0.30	0.27	0.20	0.17	0.24	0.06	0.05	0.07	0.10	0.07	0.03	
9	0.29	0.25	0.19	0.17	0.23	0.06	0.04	0.07	0.09	0.07	0.03	
8	0.27	0.23	0.18	0.16	0.21	0.05	0.04	0.06	0.09	0.06	0.03	
7	0.23	0.21	0.17	0.16	0.19	0.03	0.03	0.06	0.08	0.06	0.03	
6	0.21	0.18	0.17	0.14	0.18	0.03	0.03	0.06	0.08	0.06	0.03	
5	0.19	0.16	0.16	0.15	0.17	0.02	0.03	0.06	0.07	0.05	0.02	
4	0.16	0.14	0.17	0.14	0.15	0.02	0.03	0.04	0.06	0.04	0.02	
3	0.17	0.11	0.15	0.14	0.14	0.03	0.03	0.03	0.06	0.04	0.02	
2	0.12	0.07	0.16	0.11	0.12	0.04	0.01	0.03	0.05	0.03	0.02	
1	0.11	0.00	0.14	0.13	0.10	0.06	0.00	0.02	0.04	0.02	0.02	

PRESSURE VS STRAIN, BIAXIAL TEST, SAMPLE 208-019-OC1-10.72

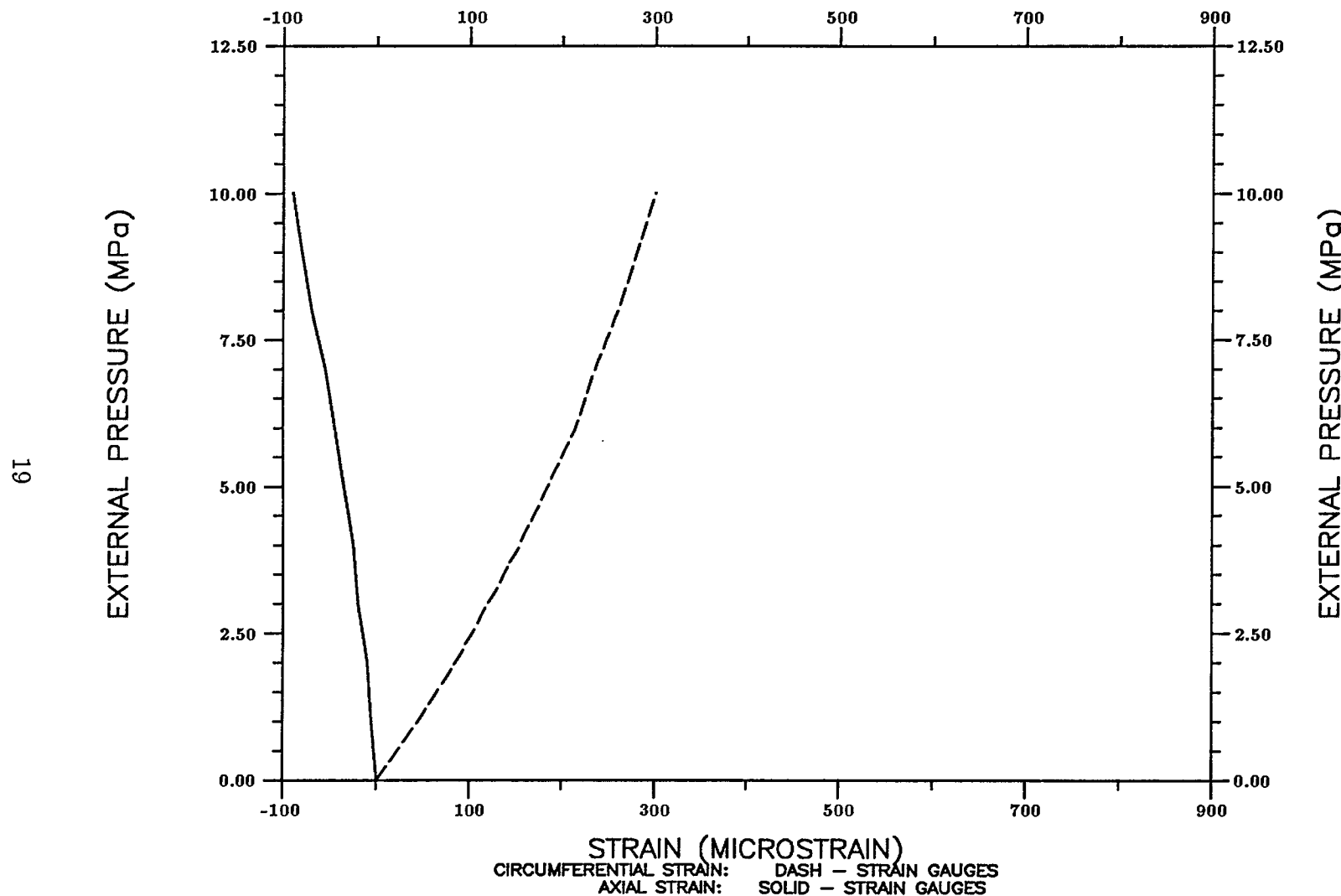


Figure 1. Plot of axial strain and circumferential strain versus external pressure for the biaxial test of Specimen 208-019-OC1-10.72.

PRESSURE VS STRAIN, BIAXIAL TEST, SAMPLE 208-019-OC1-13.54

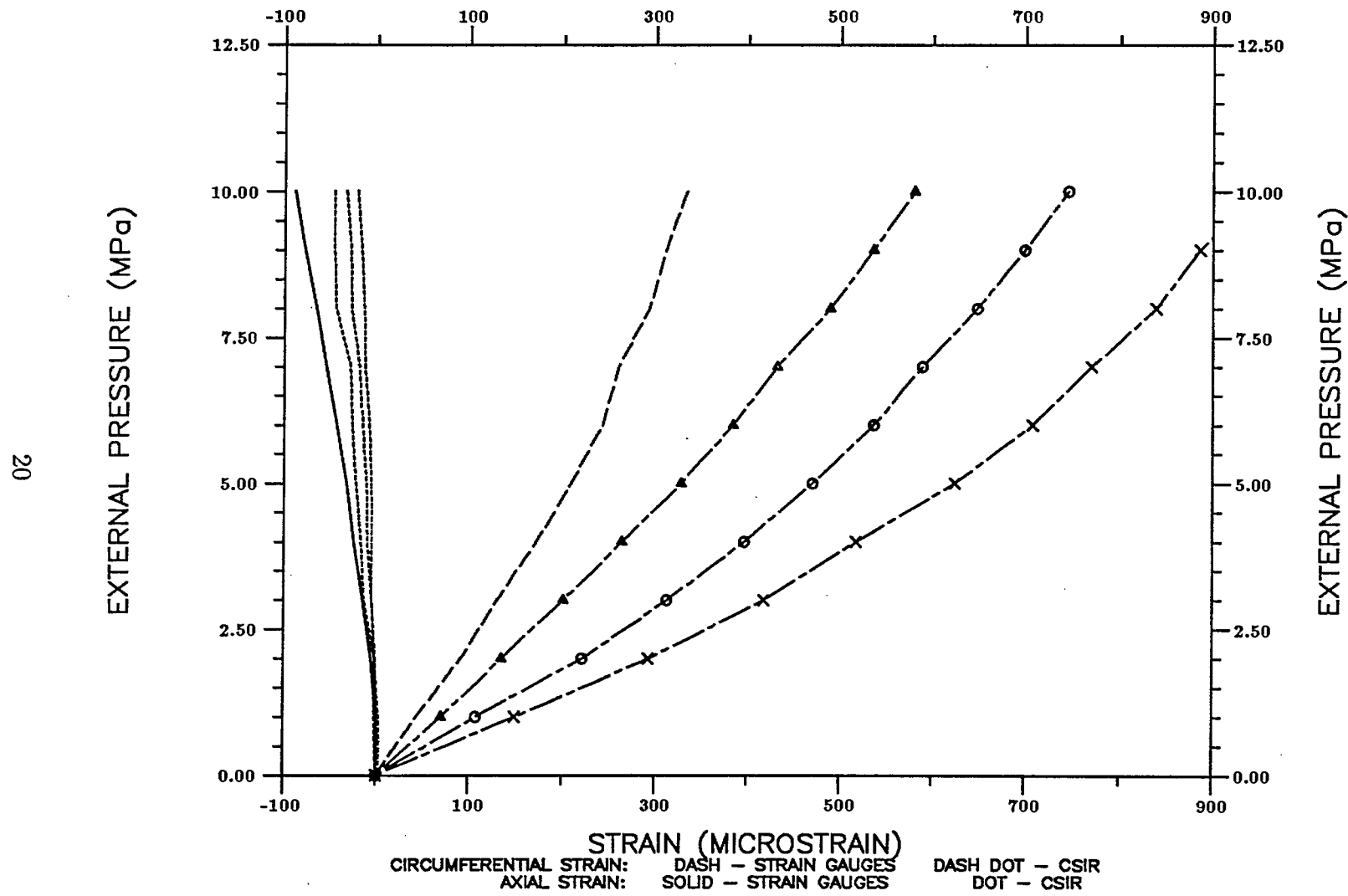


Figure 2. Plot of axial strain and circumferential strain versus external pressure for the biaxial test of Specimen 208-019-OC1-13.54 (symbols: x - e_3 , o - e_7 , triangle - e_{11}).

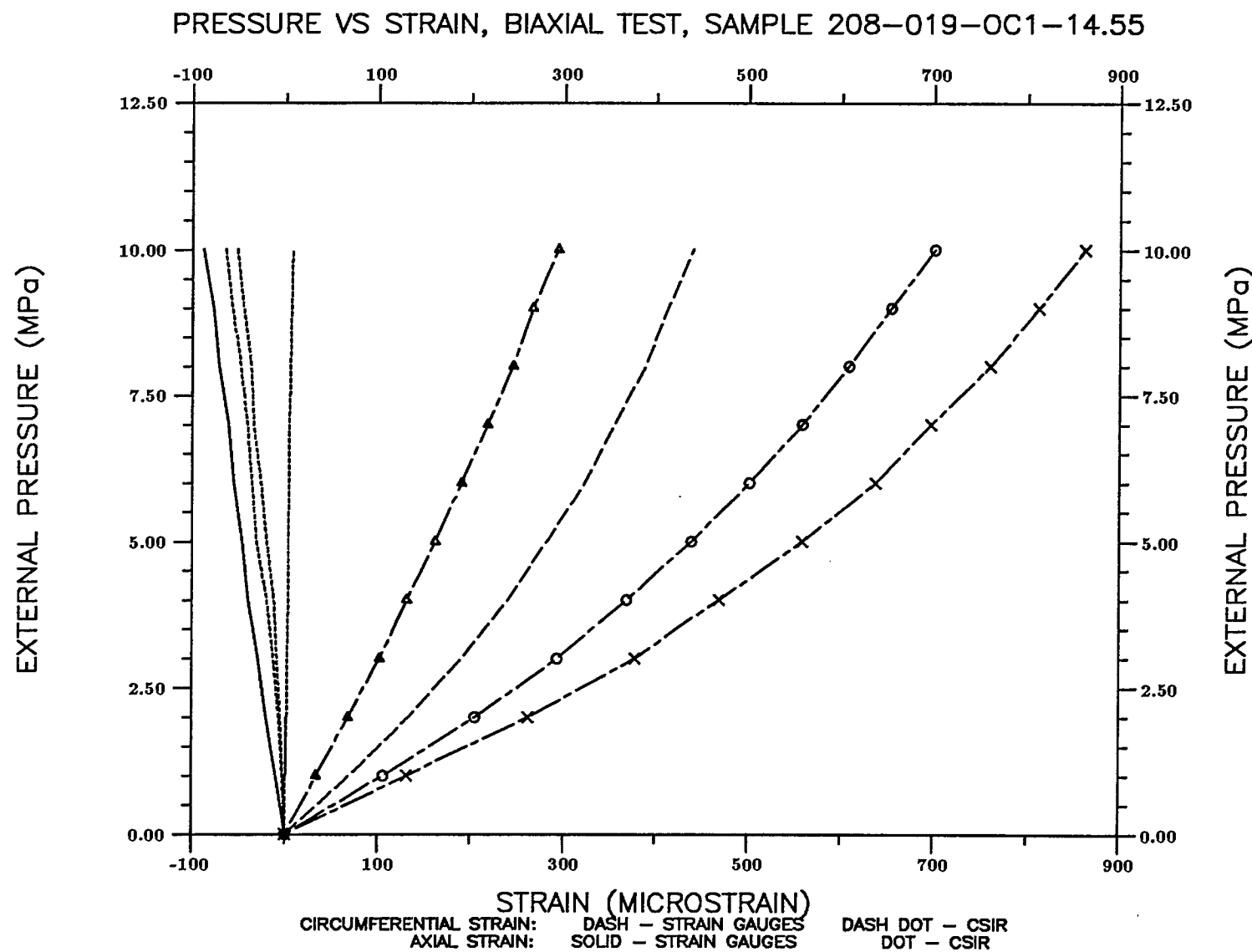


Figure 3. Plot of axial strain and circumferential strain versus external pressure for the biaxial test of Specimen 208-019-OC1-14.55 (symbols: x - e_3 , o - e_7 , triangle - e_{11}).

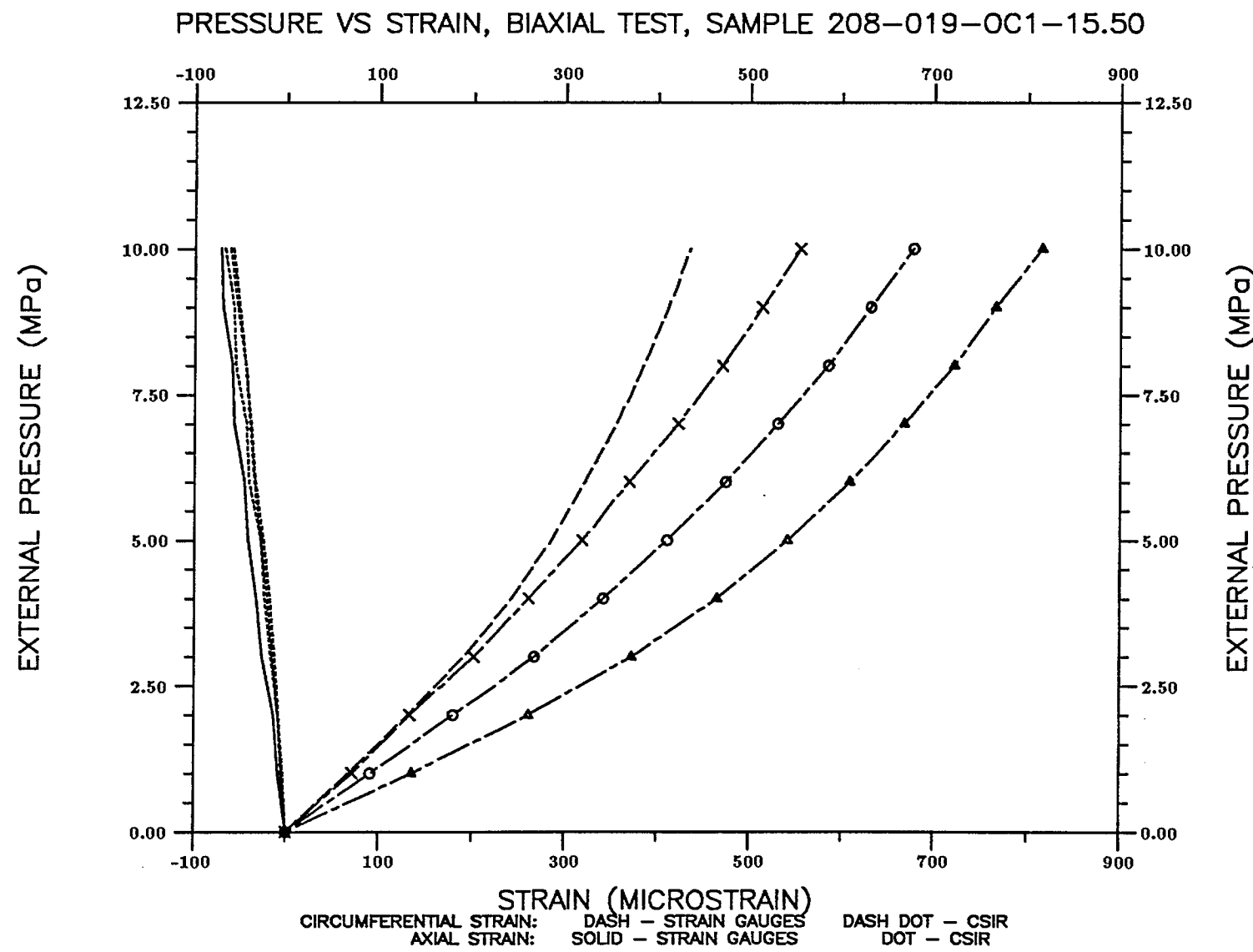


Figure 4. Plot of axial strain and circumferential strain versus external pressure for the biaxial test of Specimen 208-019-OC1-15.50 (symbols: x - e_3 , o - e_7 , triangle - e_{11}).

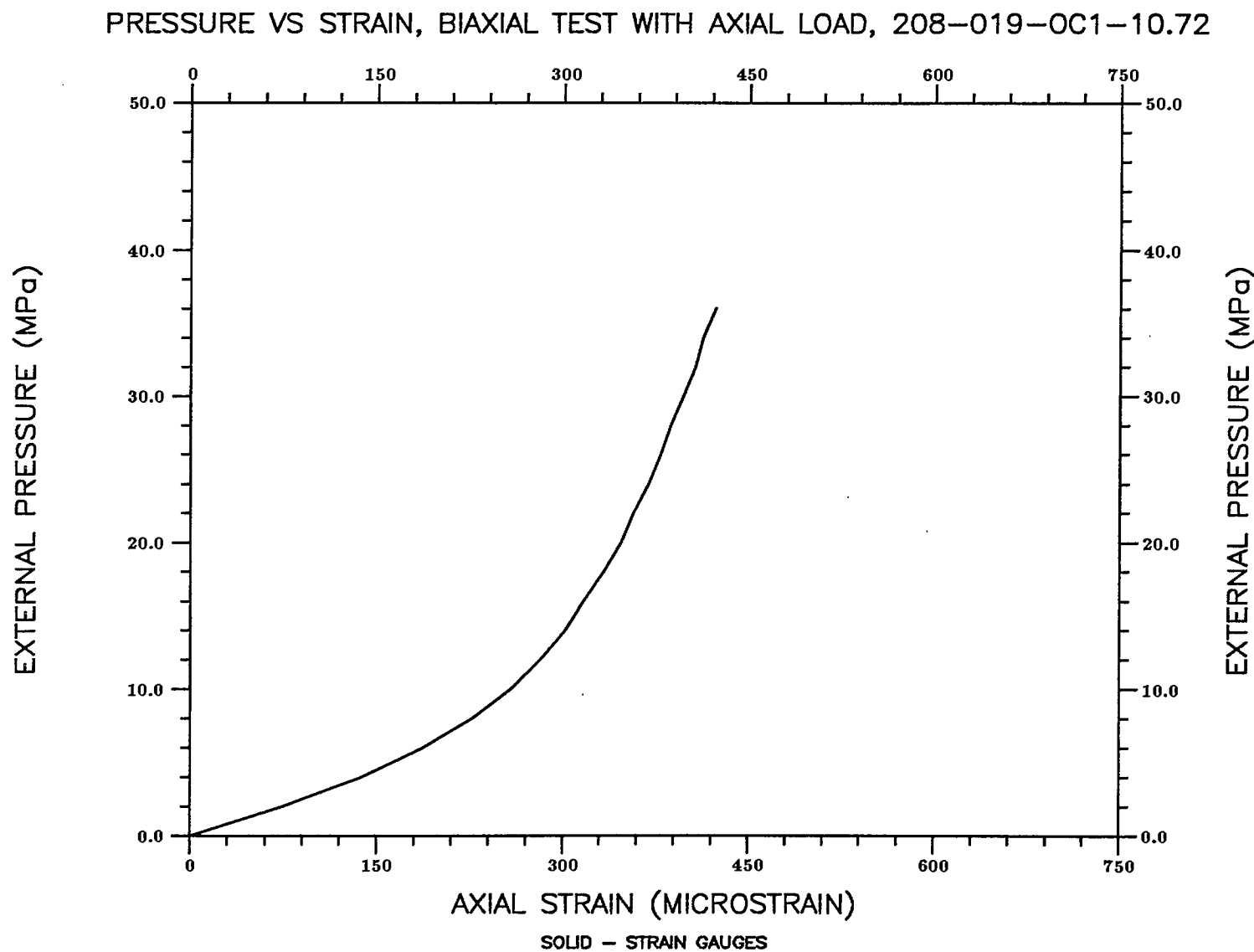


Figure 5. Plots of axial strain versus external pressure for the biaxial test with axial load of Specimen 208-019-OC1-10.72

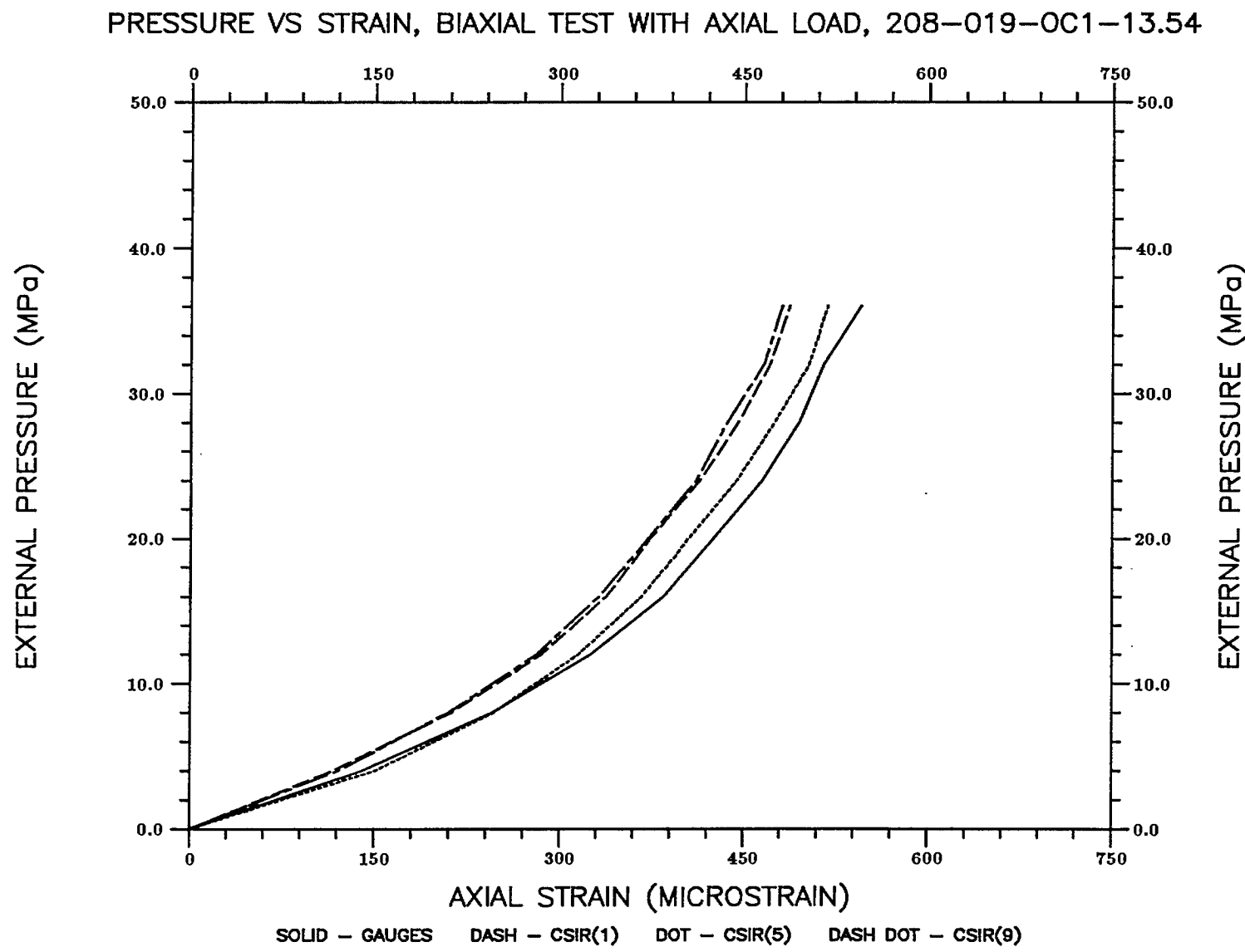


Figure 6. Plots of axial strain versus external pressure for the biaxial test with axial load of Specimen 208-019-OC1-13.54.

PRESSURE VS STRAIN, BIAXIAL TEST WITH AXIAL LOAD, 208-019-OC1-14.55

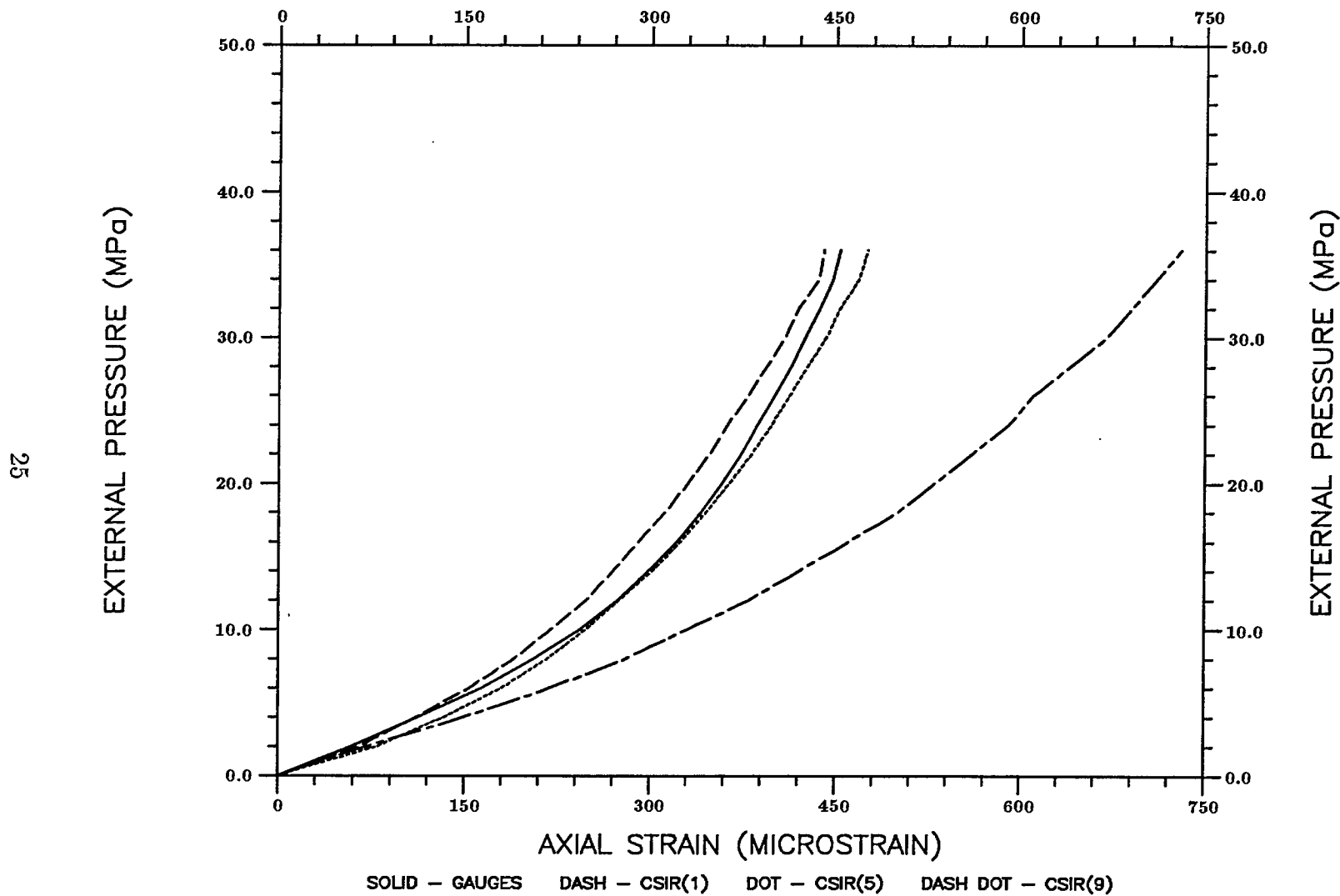


Figure 7. Plots of axial strain versus external pressure for the biaxial test with axial load of Specimen 208-019-OC1-14.55.

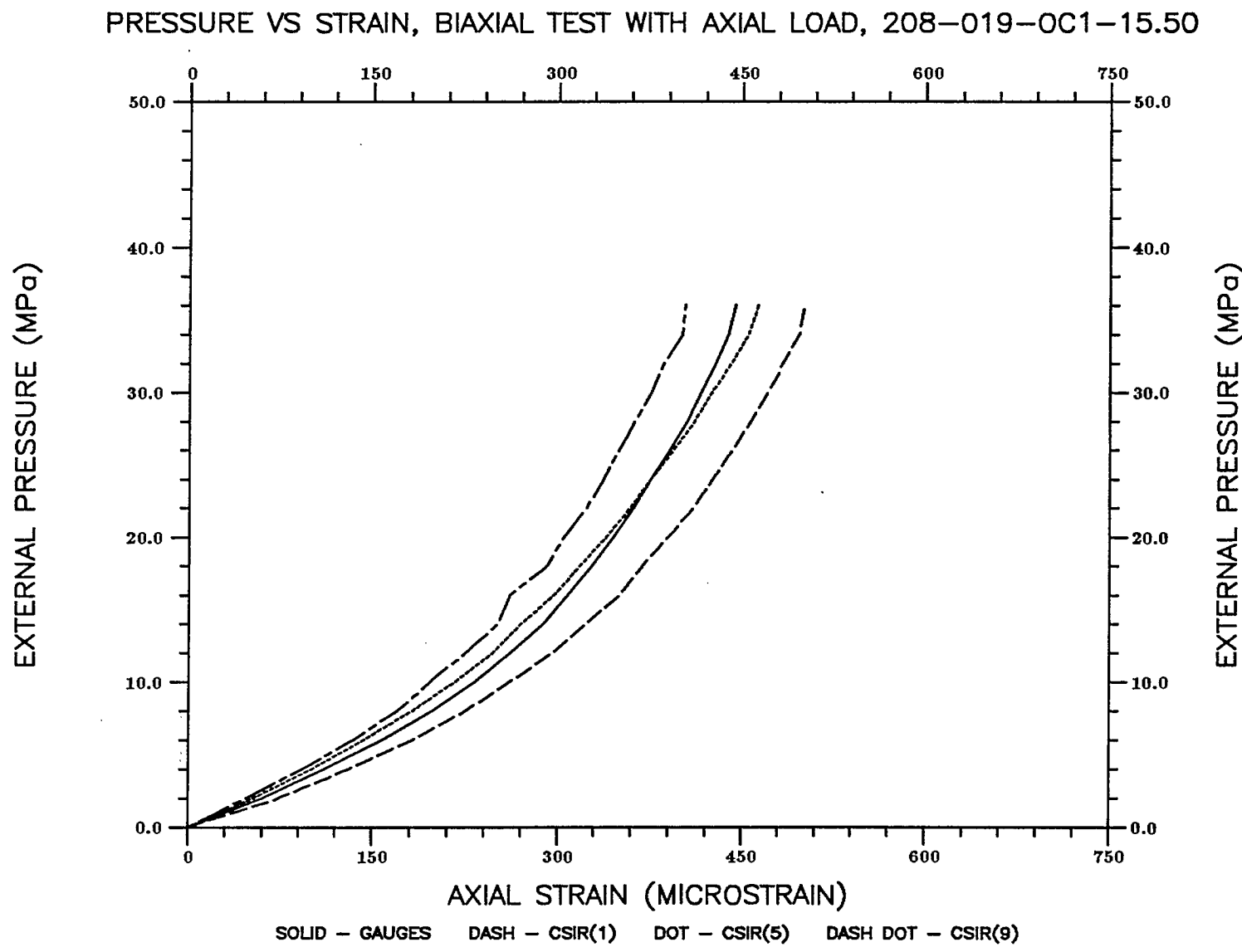


Figure 8. Plots of axial strain versus external pressure for the biaxial test with axial load of Specimen 208-019-OC1-15.50.

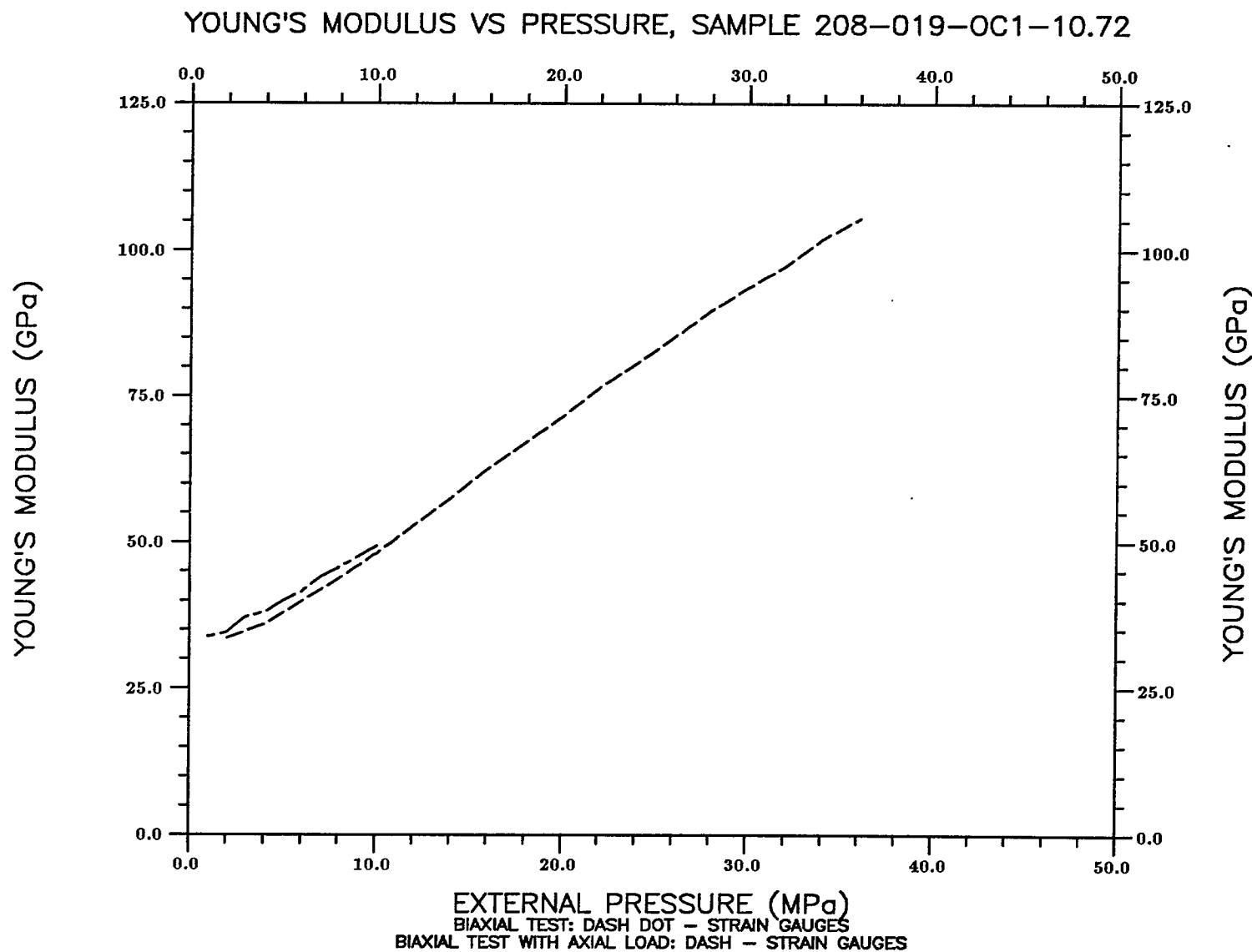


Figure 9. Plots of Young's modulus versus external pressure for Specimen 208-019-OC1-10.72

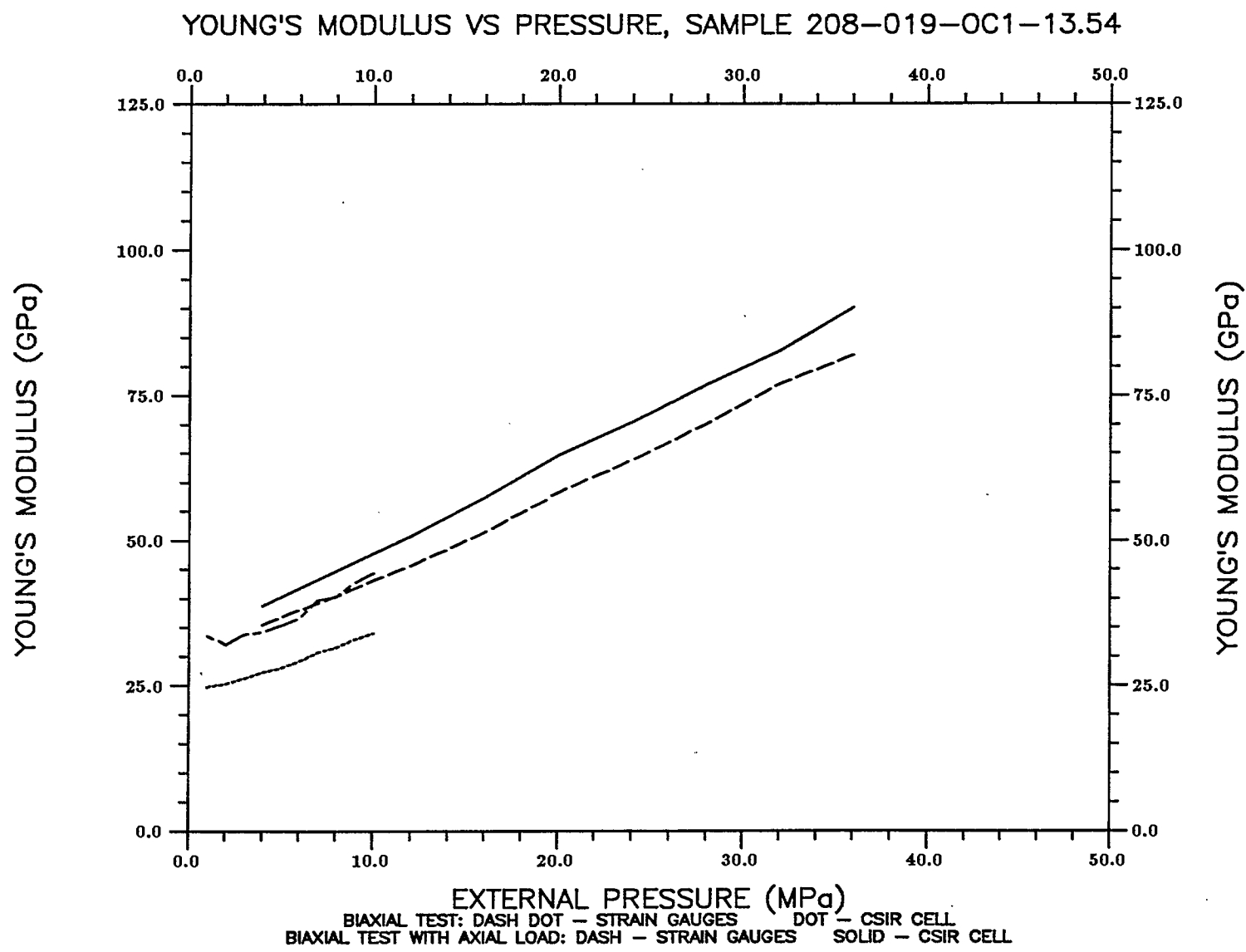


Figure 10. Plots of Young's modulus versus external pressure for Specimen 208-019-OC1-13.54

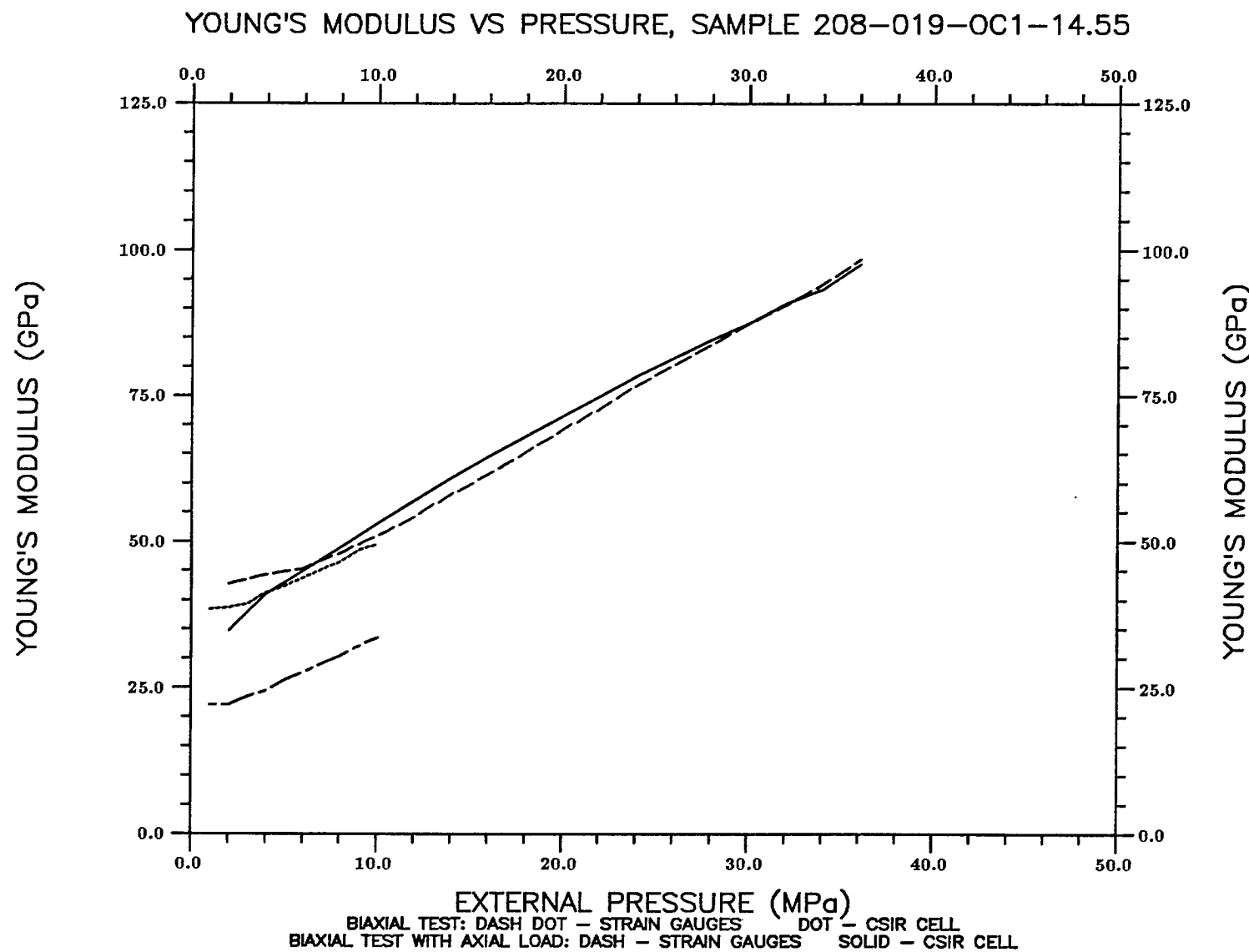


Figure 11. Plots of Young's modulus versus external pressure for Specimen 208-019-OC1-14.55

YOUNG'S MODULUS VS PRESSURE, SAMPLE 208-019-OC1-15.50

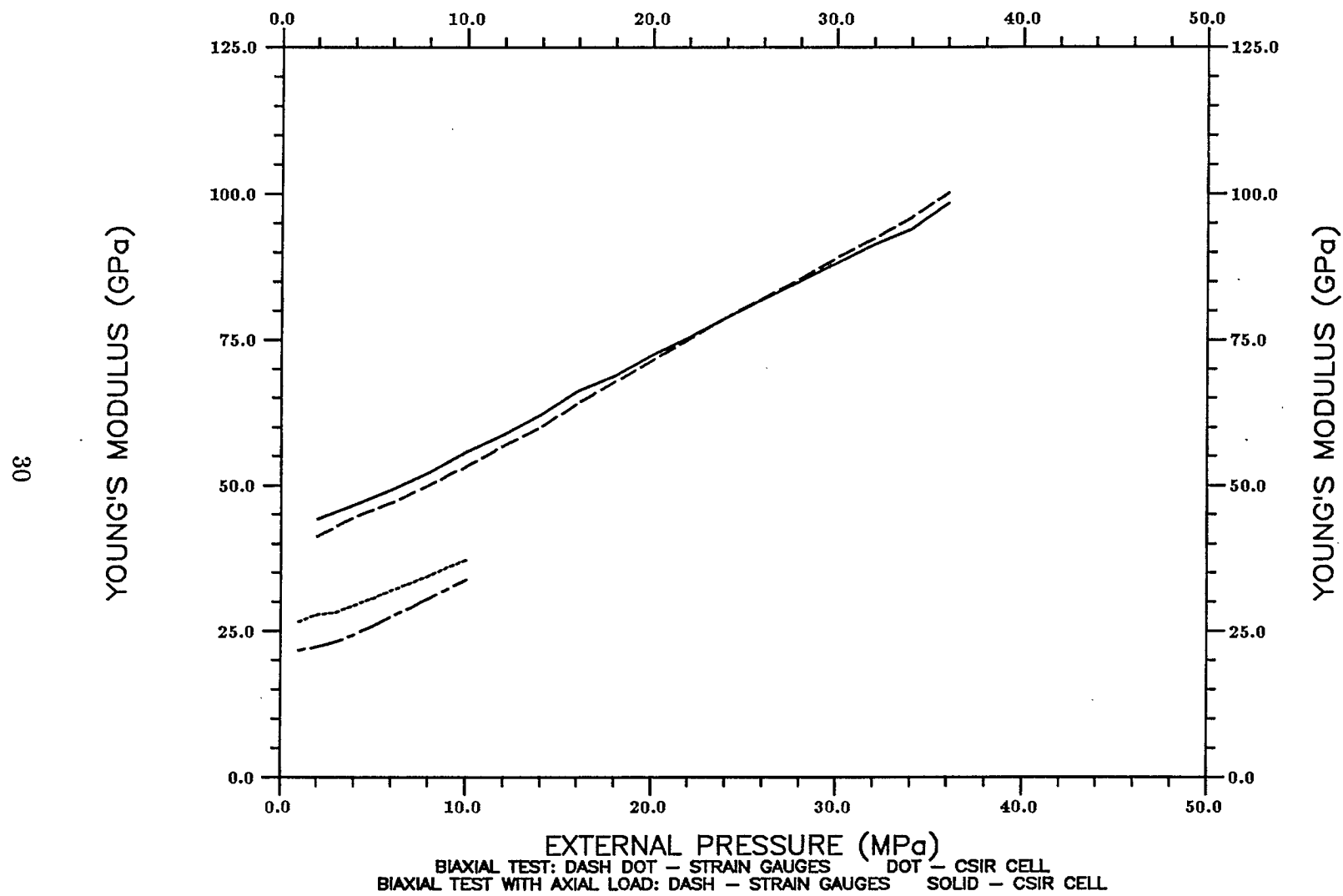


Figure 12. Plots of Young's modulus versus external pressure for Specimen 208-019-OC1-15.50

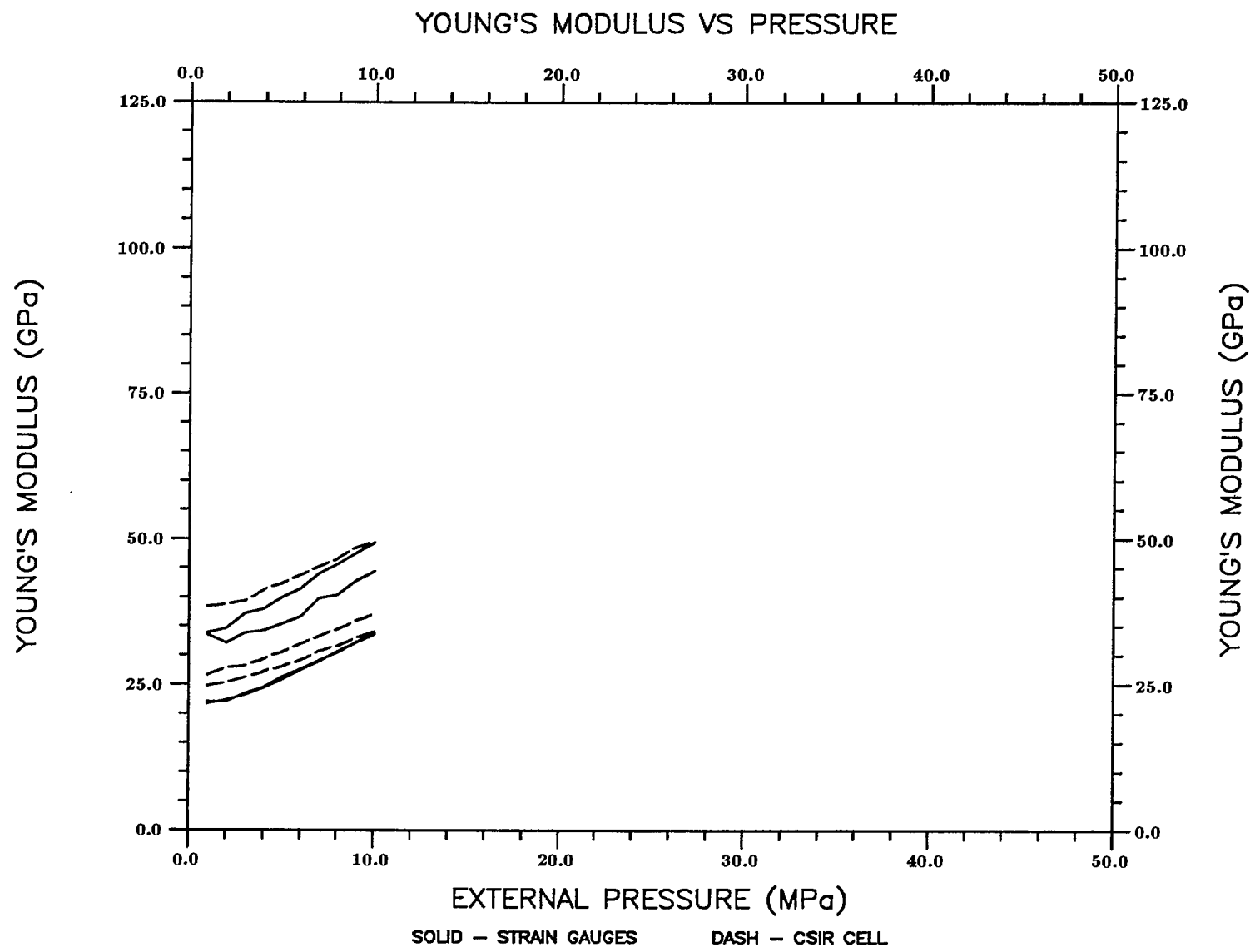


Figure 13. Plots of Young's modulus versus external pressure for the four biaxial tests.

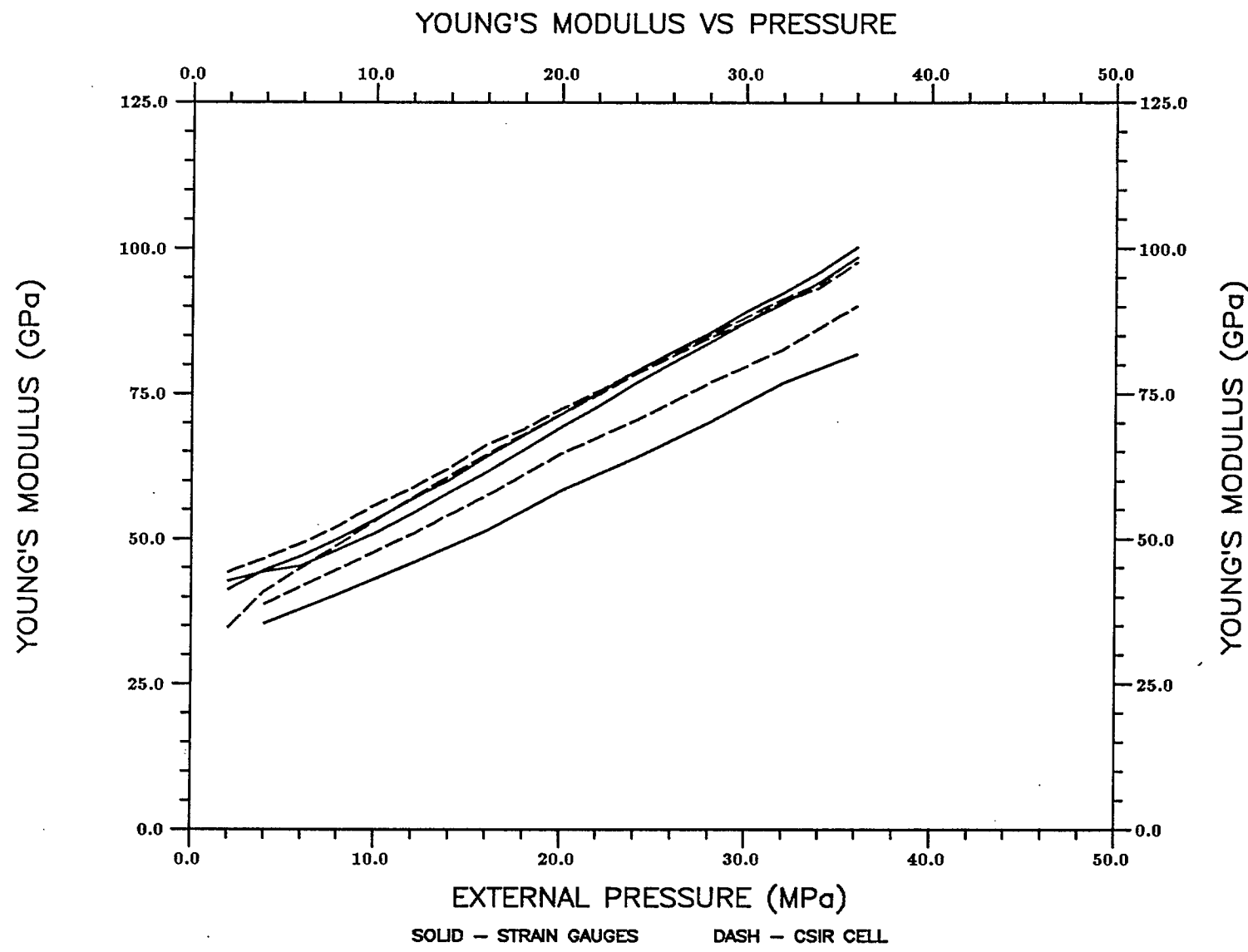


Figure 14. Plots of Young's modulus versus external pressure for the four biaxial tests with axial load.

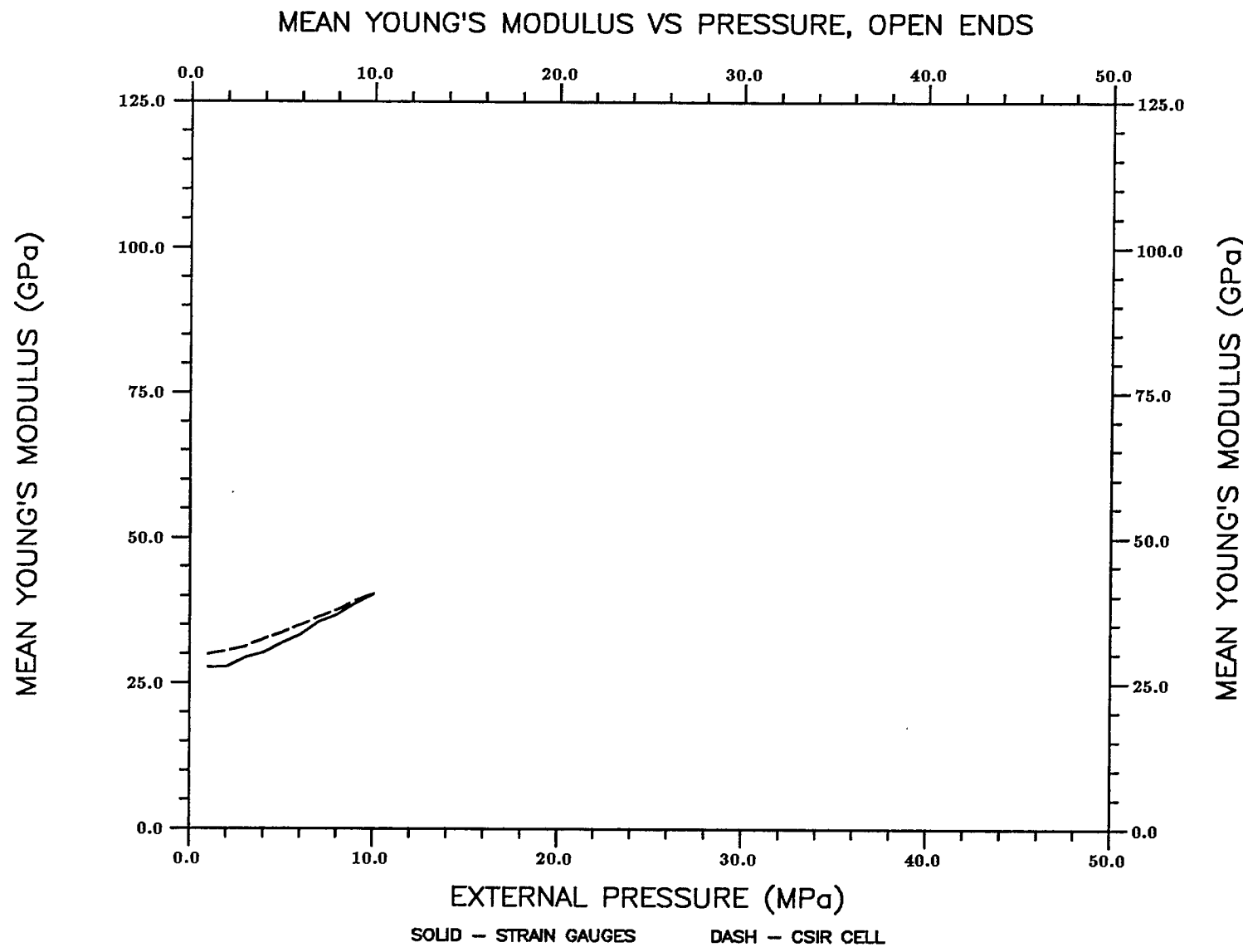


Figure 15. Plots of mean Young's modulus versus external pressure for the biaxial tests.

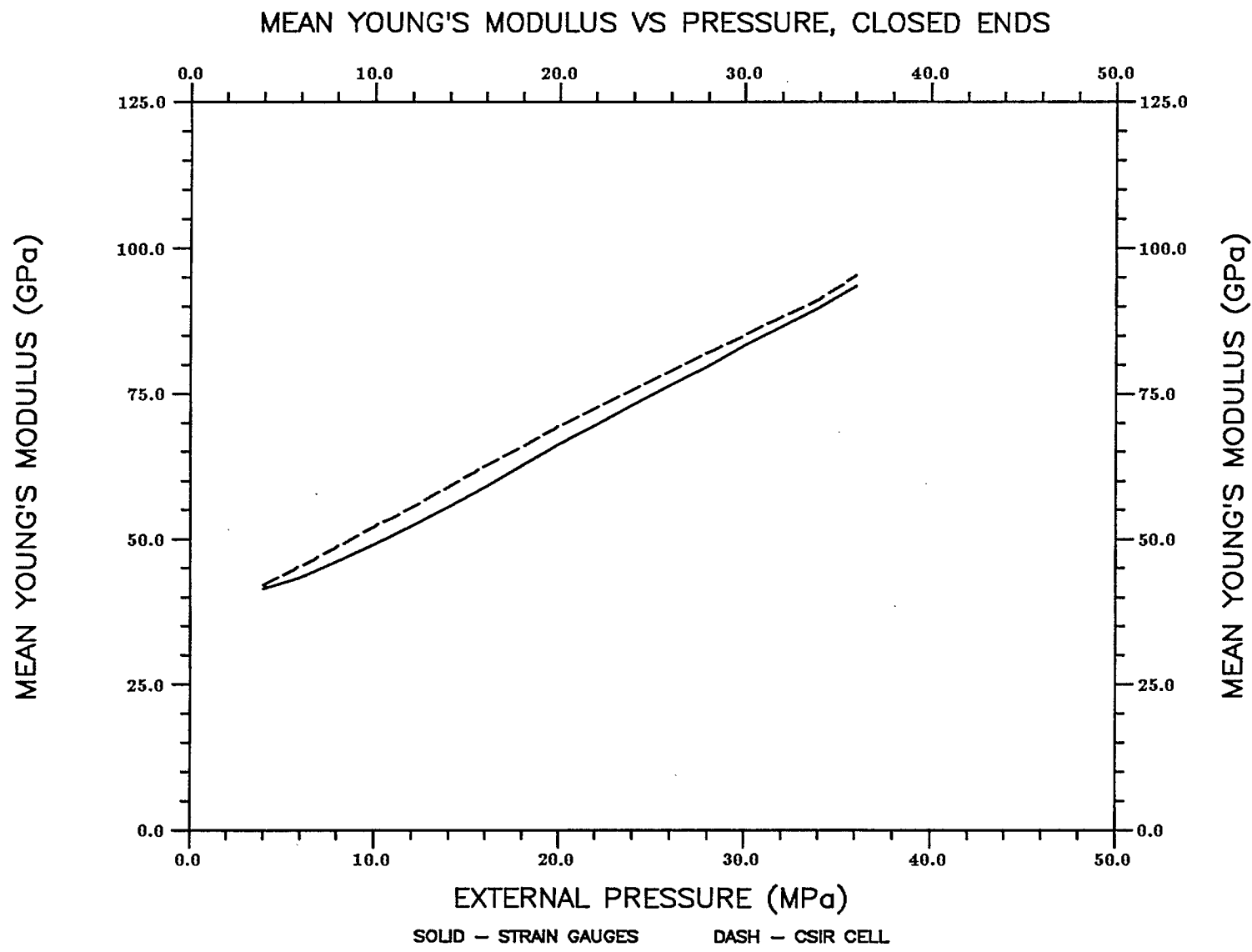


Figure 16. Plots of mean Young's modulus versus external pressure for the biaxial tests with axial load.

Appendix A

Specimen 208-019-OC1-10.72

Table A.1. Results of the biaxial test on the outside of Specimen 208-019-OC1-10.72.

P (MPa)	cycle 1				cycle 2				cycle 3			
	e_t $\times 10^6$	e_l $\times 10^6$	E (GPa)	ν	e_t $\times 10^6$	e_l $\times 10^6$	E (GPa)	ν	e_t $\times 10^6$	e_l $\times 10^6$	E (GPa)	ν
1	-55	0	27.62		-40		37.98		-35	5	43.40	0.14
2	-95	10	30.91	0.11	-75	5	39.16	0.07	-70	15	41.95	0.21
3	-130	15	34.28	0.12	-115	10	38.75	0.09	-105	20	42.44	0.19
4	-165	20	35.60	0.12	-150	15	39.16	0.10	-140	25	41.95	0.18
5	-200	30	36.96	0.15	-190	20	38.91	0.11	-170	35	43.49	0.21
6	-235	35	37.92	0.15	-220	25	40.51	0.11	-200	45	44.56	0.22
7	-265	40	38.98	0.15	-250	30	41.32	0.12	-230	50	44.91	0.22
8	-295	55	40.16	0.19	-280	35	42.32	0.13	-260	60	45.57	0.23
9	-325	60	40.82	0.18	-310	45	42.79	0.15	-285	65	46.55	0.23
10	-355	70	41.65	0.20	-340	55	43.49	0.16	-315	75	46.94	0.24
10	-320	70	46.20	0.22	-340	60	43.49	0.18	-300	90	49.28	0.30
9	-295	65	44.97	0.22	-315	55	42.12	0.17	-280	80	47.38	0.29
8	-270	55	43.88	0.20	-290	45	40.86	0.16	-260	70	45.57	0.27
7	-245	45	42.16	0.18	-265	35	38.98	0.13	-235	55	43.96	0.23
6	-220	40	40.51	0.18	-235	30	37.92	0.13	-215	45	41.45	0.21
5	-190	30	38.91	0.16	-205	20	36.06	0.10	-185	35	39.96	0.19
4	-160	25	36.71	0.16	-170	15	34.55	0.09	-155	25	37.89	0.16
3	-125	15	35.65	0.12	-135	10	33.01	0.07	-120	20	37.13	0.17
2	-90	10	32.63	0.11	-90	5	32.63	0.06	-85	10	34.55	0.12
1	-45	5	33.76	0.11	-55	5	27.62	0.09	-45	5	33.76	0.11

Table A.2. Results of the biaxial test with axial load on the outside of Specimen 208-019-OC1-10.72

loading	cycle 1		cycle 2		cycle 3		unloading	cycle 1		cycle 2		cycle 3	
	P (MPa)	e_l $\times 10^6$	E (GPa)	e_l $\times 10^6$	E (GPa)	e_l $\times 10^6$	E (GPa)	P (MPa)	e_l $\times 10^6$	E (GPa)	e_l $\times 10^6$	E (GPa)	e_l $\times 10^6$
2	-31	79.95	-35	70.82	-38	65.22	36	-428	104.24	-433	103.03	-423	105.47
4	-87	56.98	-86	57.64	-88	56.33	34	-426	98.91	-431	97.76	-413	102.02
6	-139	53.49	-133	55.91	-137	54.27	32	-415	95.56	-421	94.20	-407	97.44
8	-185	53.59	-176	56.33	-183	54.18	30	-405	91.80	-411	90.46	-397	93.65
10	-225	55.08	-216	57.37	-220	56.33	28	-398	87.18	-403	86.10	-387	89.66
12	-266	55.91	-247	60.21	-252	59.01	26	-388	83.04	-393	81.99	-379	85.02
14	-296	58.61	-271	64.02	-281	61.74	24	-376	79.10	-383	77.66	-369	80.60
16	-326	60.82	-292	67.91	-304	65.22	22	-364	74.90	-370	73.69	-357	76.37
18	-346	64.47	-309	72.19	-324	68.85	20	-351	70.61	-357	69.43	-347	71.43
20	-365	67.91	-323	76.74	-342	72.47	18	-341	65.42	-344	64.85	-333	66.99
22	-379	71.94	-335	81.39	-359	75.94	16	-325	61.01	-329	60.27	-317	62.55
24	-386	77.05	-346	85.96	-370	80.39	14	-309	56.15	-312	55.61	-302	57.45
26	-396	81.37	-356	90.51			12	-285	52.18	-290	51.28	-282	52.73
28	-398	87.18	-366	94.81	-395	87.85	10	-261	47.48	-262	47.30	-258	48.03
30	-406	91.57	-376	98.88	-404	92.03	8	-231	42.92	-230	43.11	-227	43.67
32	-409	96.96	-386	102.74	-412	96.25	6	-191	38.93	-189	39.34	-187	39.76
34	-416	101.29	-391	107.76	-416	101.29	4	-139	35.66	-139	35.66	-138	35.92
36	-403	110.70	-393	113.52	-411	108.55	2	-74	33.49	-77	32.19	-74	33.49

Appendix B

Specimen 208-019-OC1-13.54

Table B.1. Results of the biaxial test on the outside of Specimen 208-019-OC1-13.54

P (MPa)	cycle 1				cycle 2				cycle 3			
	e_t $\times 10^6$	e_l $\times 10^6$	E (GPa)	ν	e_t $\times 10^6$	e_l $\times 10^6$	E (GPa)	ν	e_t $\times 10^6$	e_l $\times 10^6$	E (GPa)	ν
1	-31	15	47.62	0.48	-36	7	41.01	0.19	-36	1	41.01	0.03
2	-68	25	43.42	0.37	-79	16	37.38	0.20	-74	9	39.90	0.12
3	-109	39	40.63	0.36	-116	24	38.18	0.21	-115	19	38.51	0.17
4	-145	48	40.73	0.33	-153	34	38.60	0.22	-152	27	38.85	0.18
5	-187	56	39.47	0.30	-186	43	39.69	0.23	-190	38	38.85	0.20
6	-224	60	39.55	0.27	-226	52	39.20	0.23	-226	43	39.20	0.19
7	-261	68	39.60	0.26	-256	59	40.37	0.23	-263	52	39.29	0.20
8	-293	74	40.31	0.25	-290	69	40.73	0.24	-292	58	40.45	0.20
9	-328	83	40.51	0.25	-319	74	41.65	0.23	-324	68	41.01	0.21
10	-358	87	41.24	0.24	-350	83	42.18	0.24	-351	73	42.06	0.21
10	-335	89	44.07	0.27	-367	70	40.23	0.19	-333	89	44.34	0.27
9	-314	82	42.32	0.26	-340	60	39.08	0.18	-311	78	42.72	0.25
8	-288	69	41.01	0.24	-316	54	37.38	0.17	-293	66	40.31	0.23
7	-262	61	39.44	0.23	-283	45	36.52	0.16	-260	55	39.75	0.21
6	-234	48	37.86	0.21	-255	39	34.74	0.15	-242	44	36.60	0.18
5	-204	39	36.19	0.19	-215	32	34.33	0.15	-209	33	35.32	0.16
4	-167	26	35.36	0.16	-178	26	33.18	0.15	-173	25	34.14	0.14
3	-133	18	33.30	0.14	-140	15	31.64	0.11	-131	15	33.81	0.11
2	-90	4	32.81	0.04	-95	11	31.08	0.12	-92	6	32.09	0.07
1	-47	0	31.41		-47	0	31.41		-44	0	33.55	

Table B.2. Results of the first cycle of the biaxial test on the inside of Specimen 208-019-OC1-13.54

P (MPa)	e_1 $\times 10^6$	e_3 $\times 10^6$	E (GPa)	ν	e_5 $\times 10^6$	e_7 $\times 10^6$	E (GPa)	ν	e_9 $\times 10^6$	e_{11} $\times 10^6$	E (GPa)	ν	E_{av} (GPa)	ν_{av}
1	9	-102	24.28	0.09	5	-87	28.46	0.06	0	-53	46.72	0.00	33.15	0.05
2	12	-236	20.99	0.05	6	-186	26.63	0.03	4	-114	43.44	0.04	30.35	0.03
3	15	-365	20.35	0.04	9	-278	26.72	0.03	2	-178	41.74	0.01	29.60	0.03
4	21	-477	20.77	0.04	12	-367	26.99	0.03	2	-240	41.27	0.01	29.68	0.03
5	24	-585	21.17	0.04	14	-448	27.64	0.03	6	-307	40.33	0.02	29.71	0.03
6	30	-681	21.82	0.04	20	-525	28.30	0.04	7	-367	40.49	0.02	30.20	0.03
7	40	-766	22.63	0.05	23	-595	29.13	0.04	9	-431	40.22	0.02	30.66	0.04
8	44	-844	23.47	0.05	27	-661	29.97	0.04	11	-490	40.43	0.02	31.29	0.04
9	49	-911	24.46	0.05	32	-719	31.00	0.04	13	-544	40.97	0.02	32.14	0.04
10	53	-977	25.35	0.05	35	-779	31.79	0.04	16	-598	41.41	0.03	32.85	0.04
Cycle 1														
10	47	-942	26.29	0.05	35	-743	33.33	0.05	19	-580	42.70	0.03	34.11	0.04
9	41	-894	24.93	0.05	31	-694	32.11	0.04	15	-536	41.58	0.03	32.87	0.04
8	37	-838	23.64	0.04	27	-645	30.71	0.04	10	-487	40.68	0.02	31.68	0.03
7	31	-776	22.34	0.04	22	-589	29.43	0.04	7	-438	39.58	0.02	30.45	0.03
6	25	-707	21.02	0.04	17	-532	27.93	0.03	3	-387	38.39	0.01	29.11	0.03
5	22	-626	19.78	0.04	14	-466	26.57	0.03	1	-324	38.22	0.00	28.19	0.02
4	14	-531	18.65	0.03	10	-390	25.40	0.03	0	-265	37.38	0.00	27.14	0.02
3	9	-425	17.48	0.02	6	-314	23.66	0.02	0	-203	36.60	0.00	25.91	0.01
2	6	-280	17.69	0.02	4	-216	22.93	0.02	-1	-135	36.69	0.00	25.77	0.01
1	3	-149	16.62	0.02	2	-112	22.11	0.02	-1	-68	36.42	0.00	25.05	0.01

Table B.3. Results of the second cycle of the biaxial test on the inside of Specimen 208-019-OC1-13.54

P (MPa)	e_1 $\times 10^6$	e_3 $\times 10^6$	E (GPa)	ν	e_5 $\times 10^6$	e_7 $\times 10^6$	E (GPa)	ν	e_9 $\times 10^6$	e_{11} $\times 10^6$	E (GPa)	ν	E_{av} (GPa)	ν_{av}
1	6	-115	21.53	0.05	9	-85	29.13	0.11	1	-54	45.86	0.02	32.17	0.06
2	12	-234	21.17	0.05	10	-179	27.67	0.06	6	-112	44.22	0.05	31.02	0.05
3	14	-360	20.64	0.04	13	-268	27.72	0.05	7	-172	43.19	0.04	30.52	0.04
4	20	-471	21.03	0.04	15	-355	27.90	0.04	8	-236	41.97	0.03	30.30	0.04
5	25	-568	21.80	0.04	17	-432	28.66	0.04	9	-301	41.14	0.03	30.53	0.04
6	33	-658	22.58	0.05	21	-502	29.60	0.04	11	-360	41.27	0.03	31.15	0.04
7	37	-743	23.33	0.05	27	-568	30.52	0.05	13	-418	41.47	0.03	31.77	0.04
8	42	-816	24.28	0.05	31	-628	31.55	0.05	15	-476	41.62	0.03	32.48	0.04
9	45	-879	25.36	0.05	34	-685	32.54	0.05	19	-527	42.29	0.04	33.40	0.05
10	53	-945	26.20	0.06	38	-742	33.37	0.05	22	-577	42.92	0.04	34.16	0.05
Cycle 2														
10	58	-951	26.04	0.06	42	-738	33.56	0.06	27	-573	43.22	0.05	34.27	0.06
9	50	-898	24.82	0.06	38	-692	32.21	0.05	20	-531	41.97	0.04	33.00	0.05
8	43	-845	23.44	0.05	30	-642	30.86	0.05	16	-485	40.85	0.03	31.72	0.04
7	38	-784	22.11	0.05	27	-589	29.43	0.05	12	-437	39.67	0.03	30.40	0.04
6	29	-715	20.78	0.04	20	-533	27.88	0.04	12	-384	38.69	0.03	29.12	0.04
5	22	-638	19.41	0.03	18	-466	26.57	0.04	3	-326	37.98	0.01	27.99	0.03
4	16	-534	18.55	0.03	12	-395	25.08	0.03	2	-264	37.52	0.01	27.05	0.02
3	12	-438	16.96	0.03	9	-316	23.51	0.03	1	-205	36.24	0.00	25.57	0.02
2	9	-301	16.45	0.03	5	-216	22.93	0.02	-2	-135	36.69		25.36	0.02
1	1	-163	15.19	0.01	1	-112	22.11	0.01	0	-69	35.89	0.00	24.40	0.01

Table B.4. Results of the third cycle of the biaxial test on the inside of Specimen 208-019-OC1-13.54

P (MPa)	e_1 $\times 10^6$	e_3 $\times 10^6$	E (GPa)	ν	e_5 $\times 10^6$	e_7 $\times 10^6$	E (GPa)	ν	e_9 $\times 10^6$	e_{11} $\times 10^6$	E (GPa)	ν	E_{av} (GPa)	ν_{av}
1	7	-126	19.65	0.06	9	-86	28.79	0.10	2	-54	45.86	0.04	31.43	0.07
2	15	-249	19.89	0.06	11	-182	27.21	0.06	5	-112	44.22	0.04	30.44	0.05
3	16	-372	19.97	0.04	13	-273	27.21	0.05	7	-173	42.94	0.04	30.04	0.04
4	23	-485	20.42	0.05	17	-354	27.98	0.05	9	-238	41.62	0.04	30.01	0.05
5	28	-586	21.13	0.05	22	-433	28.60	0.05	12	-300	41.27	0.04	30.33	0.05
6	33	-676	21.98	0.05	23	-506	29.36	0.05	14	-357	41.62	0.04	30.99	0.05
7	38	-755	22.96	0.05	28	-571	30.36	0.05	15	-418	41.47	0.04	31.60	0.05
8	46	-822	24.10	0.06	31	-632	31.35	0.05	17	-475	41.71	0.04	32.39	0.05
9	54	-890	25.04	0.06	37	-688	32.39	0.05	21	-527	42.29	0.04	33.24	0.05
10	54	-954	25.96	0.06	42	-741	33.42	0.06	26	-576	42.99	0.05	34.12	0.06
Cycle 3														
10	45	-947	26.15	0.05	34	-745	33.24	0.05	22	-580	42.70	0.04	34.03	0.05
9	47	-886	25.15	0.05	29	-699	31.88	0.04	17	-535	41.66	0.03	32.90	0.04
8	45	-839	23.61	0.05	28	-648	30.57	0.04	14	-489	40.51	0.03	31.56	0.04
7	29	-770	22.51	0.04	19	-589	29.43	0.03	13	-432	40.13	0.03	30.69	0.03
6	27	-708	20.99	0.04	16	-536	27.72	0.03	8	-384	38.69	0.02	29.13	0.03
5	23	-624	19.84	0.04	11	-470	26.34	0.02	6	-328	37.75	0.02	27.98	0.03
4	14	-517	19.16	0.03	10	-397	24.95	0.03	5	-264	37.52	0.02	27.21	0.03
3	17	-418	17.77	0.04	5	-313	23.74	0.02	5	-201	36.96	0.02	26.16	0.03
2	2	-293	16.90	0.01	2	-221	22.41	0.01	1	-136	36.42	0.01	25.24	0.01
1	-3	-150	16.51		2	-108	22.93	0.02	0	-71	34.88	0.00	24.77	0.00

Table B.5. Results of the biaxial test with axial load on the outside of Specimen 208-019-OC1-13.54

loading	cycle 1		cycle 2		cycle 3		unloading	cycle 1		cycle 2		cycle 3		
	P (MPa)	e_l $\times 10^6$	E (GPa)	e_l $\times 10^6$	E (GPa)	e_l $\times 10^6$	E (GPa)	P (MPa)	e_l $\times 10^6$	E (GPa)	e_l $\times 10^6$	E (GPa)	e_l $\times 10^6$	E (GPa)
2	-65	38.10	-30	82.55				36			-515	86.55	-545	81.79
4	-105	47.17	-70	70.75	-60	82.55		34	-555	75.85	-500	84.20		
6	-155	47.93	-115	64.60				32	-545	72.70	-495	80.04	-515	76.94
8	-200	49.53	-160	61.91	-160	61.91		30	-530	70.09	-475	78.20		
10	-245	50.54	-205	60.40				28	-520	66.67	-465	74.56	-495	70.04
12	-280	53.06	-245	60.65	-240	61.91		26	-505	63.75	-450	71.54		
14	-330	52.53	-280	61.91				24	-490	60.65	-435	68.31	-465	63.91
16	-365	54.28	-315	62.89	-320	61.91		22	-475	57.35	-420	64.86		
18	-400	55.72	-345	64.60				20	-450	55.03	-400	61.91	-425	58.27
20	-430	57.59	-375	66.04	-380	65.17		18	-430	51.83	-380	58.65		
22	-450	60.53	-395	68.96				16	-410	48.32	-360	55.03	-385	51.46
24	-480	61.91	-415	71.61	-420	70.75		14	-390	44.45	-330	52.53		
26	-500	64.39	-440	73.17				12	-360	41.27	-300	49.53	-325	45.72
28	-525	66.04	-455	76.20	-460	75.37		10	-325	38.10	-260	47.62		
30	-545	68.16	-475	78.20				8	-290	34.16	-225	44.02	-245	40.43
32	-565	70.13	-495	80.04	-500	79.24		6	-240	30.95	-180	41.27		
34	-585	71.96	-515	81.74				4	-190	26.07	-120	41.27	-140	35.38
36			-535	83.32	-530	84.10		2	-130	19.05	-60	41.27		

Table B.6. Results of the first cycle of the biaxial test with axial load on the inside of Specimen 208-019-OC1-13.54

P (MPa)	e_1 $\times 10^6$	E (GPa)	e_5 $\times 10^6$	E (GPa)	e_9 $\times 10^6$	E (GPa)	E_{av} (GPa)	P (MPa)	e_1 $\times 10^6$	E (GPa)	e_5 $\times 10^6$	E (GPa)	e_9 $\times 10^6$	E (GPa)	E_{av} (GPa)
2	-40	61.91	-95	26.07	-63	39.31	42.43	35	-485	89.35	-537	80.70	-469	92.40	87.48
4	-76	65.17	-149	33.24	-107	46.29	48.23	34	-487	86.44	-539	78.10	-466	90.34	84.96
6	-118	62.96	-194	38.29	-142	52.32	51.19	32	-474	83.59	-526	75.33	-453	87.47	82.13
8	-160	61.91	-239	41.45	-188	52.69	52.02	30	-461	80.58	-512	72.55	-442	84.04	79.06
10	-201	61.60	-278	44.54	-226	54.79	53.64	28	-448	77.39	-499	69.48	-427	81.19	76.02
12	-240	61.91	-314	47.32	-256	58.04	55.76	26	-431	74.69	-483	66.65	-415	77.57	72.97
14	-274	63.26	-345	50.25	-289	59.98	57.83	24	-418	71.09	-468	63.50	-403	73.74	69.44
16	-307	64.53	-376	52.69	-315	62.89	60.04	22	-401	67.93	-452	60.27	-386	70.57	66.26
18	-341	65.36	-405	55.03	-341	65.36	61.92	20	-382	64.83	-433	57.19	-363	68.22	63.41
20	-364	68.03	-427	57.99	-366	67.66	64.56	18	-364	61.23	-415	53.70	-351	63.50	59.48
22	-388	70.21	-448	60.80	-387	70.39	67.13	16	-341	58.10	-388	51.06	-327	60.58	56.58
24	-413	71.95	-474	62.69	-411	72.30	68.98	14	-322	53.83	-371	46.72	-306	56.65	52.40
26	-434	74.18	-493	65.30	-426	75.57	71.68	12	-293	50.71	-344	43.19	-283	52.50	48.80
28	-453	76.53	-512	67.71	-443	78.26	74.17	10	-265	46.72	-309	40.07	-250	49.53	45.44
30	-472	78.70	-532	69.82	-461	80.58	76.37	8	-228	43.44	-280	35.38	-217	45.65	41.49
32	-491	80.70	-549	72.17	-478	82.89	78.59	6	-190	39.10	-239	31.08	-178	41.74	37.31
34	-508	82.87	-563	74.77	-497	84.70	80.78	4	-141	35.13	-186	26.63	-134	36.96	32.91
35	-515	84.15	-571	75.90	-505	85.81	81.95	2	-88	28.14	-131	18.90	-82	30.20	25.75

Table B.7. Results of the second cycle of the biaxial test with axial load on the inside of Specimen 208-019-OC1-13.54

P (MPa)	e_1 $\times 10^6$	E (GPa)	e_5 $\times 10^6$	E (GPa)	e_9 $\times 10^6$	E (GPa)	E_{av} (GPa)	P (MPa)	e_1 $\times 10^6$	E (GPa)	e_5 $\times 10^6$	E (GPa)	e_9 $\times 10^6$	E (GPa)	E_{av} (GPa)
2	-20	123.82	-57	43.44	-56	44.22	70.49	36	-481	92.67	-495	90.05	-472	94.44	92.39
4	-57	86.89	-106	46.72	-99	50.03	61.21	34	-478	88.07	-489	86.09	-463	90.92	88.36
6	-102	72.83	-151	49.20	-139	53.45	58.49	32	-463	85.58	-477	83.06	-449	88.24	85.63
8	-143	69.27	-192	51.59	-180	55.03	58.63	30	-450	82.55	-459	80.93	-440	84.42	82.63
10	-182	68.03	-231	53.60	-218	56.80	59.48	28	-436	79.52	-448	77.39	-421	82.35	79.75
12	-222	66.93	-268	55.44	-248	59.91	60.76	26	-422	76.29	-429	75.04	-402	80.08	77.14
14	-254	68.25	-297	58.37	-280	61.91	62.84	24	-406	73.19	-416	71.43	-392	75.81	73.48
16	-286	69.27	-328	60.40	-308	64.32	64.66	22	-390	69.85	-401	67.93	-377	72.25	70.01
18	-313	71.21	-353	63.14	-332	67.13	67.16	20	-373	66.39	-383	64.66	-356	69.56	66.87
20	-339	73.05	-376	65.86	-352	70.35	69.75	18	-352	63.32	-361	61.74	-340	65.55	63.54
22	-362	75.25	-396	68.79	-371	73.42	72.49	16	-330	60.03	-341	58.10	-315	62.89	60.34
24	-385	77.19	-417	71.26	-393	75.61	74.69	14	-305	56.83	-316	54.86	-295	58.76	56.82
26	-404	79.68	-439	73.33	-412	78.14	77.05	12	-279	53.26	-284	52.32	-266	55.86	53.81
28	-421	82.35	-457	75.86	-429	80.81	79.67	10	-246	50.33	-259	47.81	-239	51.81	49.98
30	-440	84.42	-474	78.37	-446	83.29	82.03	8	-207	47.85	-222	44.62	-201	49.28	47.25
32	-457	86.70	-490	80.86	-462	85.76	84.44	6	-164	45.30	-181	41.04	-159	46.72	44.35
34	-473	89.00	-506	83.20	-479	87.89	86.70	4	-113	43.83	-125	39.62	-108	45.86	43.10
36	-488	91.34	-521	85.56	-493	90.41	89.10	2	-58	42.70	-68	36.42	-57	43.44	40.85

Table B.8. Results of the third cycle of the biaxial test with axial load on the inside of Specimen 208-019-OC1-13.54

P (MPa)	e_1 $\times 10^6$	E (GPa)	e_5 $\times 10^6$	E (GPa)	e_9 $\times 10^6$	E (GPa)	E_{av} (GPa)	P (MPa)	e_1 $\times 10^6$	E (GPa)	e_5 $\times 10^6$	E (GPa)	e_9 $\times 10^6$	E (GPa)	E_{av} (GPa)
4	-65	76.20	-81	61.14	-74	66.93	68.09	36	-487	91.53	-518	86.05	-481	92.67	90.08
8	-151	65.60	-169	58.61	-156	63.50	62.57	32	-471	84.12	-503	78.77	-466	85.03	82.64
12	-225	66.04	-245	60.65	-232	64.04	63.58	28	-445	77.91	-475	72.99	-436	79.52	76.81
16	-288	68.79	-305	64.95	-289	68.55	67.43	24	-414	71.78	-444	66.93	-411	72.30	70.34
20	-337	73.48	-349	70.96	-333	74.37	72.94	20	-374	66.21	-405	61.14	-372	66.57	64.64
24	-381	78.00	-397	74.85	-369	80.53	77.79	16	-338	58.61	-367	53.98	-332	59.67	57.42
28	-419	82.74	-433	80.07	-407	85.18	82.66	12	-285	52.13	-315	47.17	-281	52.88	50.73
32	-454	87.27	-468	84.66	-438	90.46	87.46	8	-212	46.72	-246	40.27	-210	47.17	44.72
36	-481	92.67	-493	90.41	-467	95.45	92.84	4	-117	42.33	-151	32.80	-121	40.93	38.69

Appendix C

Specimen 208-019-OC1-14.55

Table C.1. Results of the biaxial test on the outside of Specimen 208-019-OC1-14.55

P (MPa)	cycle 1				cycle 2				cycle 3			
	e_t $\times 10^6$	e_l $\times 10^6$	E (GPa)	ν	e_t $\times 10^6$	e_l $\times 10^6$	E (GPa)	ν	e_t $\times 10^6$	e_l $\times 10^6$	E (GPa)	ν
1	-55	8	27.58	0.15	-50	13	30.33	0.26	-52	8	29.17	0.15
2	-114	19	25.72	0.17	-103	22	28.47	0.21	-109	20	26.90	0.18
3	-171	28	26.02	0.16	-160	34	27.80	0.21	-163	26	27.29	0.16
4	-223	39	26.30	0.17	-205	42	28.61	0.20	-214	37	27.40	0.17
5	-270	48	27.34	0.18	-253	53	29.17	0.21	-260	44	28.39	0.17
6	-317	62	28.07	0.20	-295	62	30.16	0.21	-303	56	29.36	0.18
7	-353	71	29.22	0.20	-332	73	31.06	0.22	-339	62	30.42	0.18
8	-392	87	30.18	0.22	-367	83	32.23	0.23	-376	74	31.46	0.20
9	-423	98	31.31	0.23	-396	91	33.45	0.23	-406	79	32.62	0.19
10	-457	115	32.30	0.25	-429	103	34.41	0.24	-437	94	33.78	0.22
10	-436	89	33.86	0.20	-427	96	34.57	0.22	-440	88	33.55	0.20
9	-408	78	32.46	0.19	-399	85	33.20	0.21	-413	77	32.07	0.19
8	-384	72	30.81	0.19	-375	80	31.55	0.21	-389	71	30.41	0.18
7	-351	61	29.38	0.17	-342	70	30.16	0.20	-355	61	29.05	0.17
6	-320	55	27.80	0.17	-311	64	28.61	0.21	-323	55	27.55	0.17
5	-280	45	26.36	0.16	-271	53	27.24	0.20	-281	46	26.27	0.16
4	-237	38	24.74	0.16	-226	47	25.95	0.21	-240	40	24.43	0.17
3	-186	28	23.92	0.15	-178	35	24.99	0.20	-190	29	23.41	0.15
2	-129	21	22.73	0.16	-124	25	23.65	0.20	-133	21	22.05	0.16
1	-63	10	24.07	0.16	-62	11	24.46	0.18	-69	10	21.98	0.14

Table C.2. Results of the first cycle of the biaxial test on the inside of Specimen 208-019-OC1-14.55

P (MPa)	e_1 $\times 10^6$	e_3 $\times 10^6$	E (GPa)	ν	e_5 $\times 10^6$	e_7 $\times 10^6$	E (GPa)	ν	e_9 $\times 10^6$	e_{11} $\times 10^6$	E (GPa)	ν	E_{av} (GPa)	ν_{av}	
1	6	-102	24.28	0.06	7	-87	28.46	0.08	3	-26	95.24		49.33	0.07	
2	11	-219	22.61	0.05	3	-178	27.82	0.02	0	-53	93.44		47.96	0.04	
3	18	-338	21.98	0.05	10	-273	27.21	0.04	-1	-87	85.39		44.86	0.05	
4	24	-436	22.72	0.06	14	-352	28.14	0.04	-1	-122	81.19		44.02	0.05	
5	30	-535	23.14	0.06	20	-435	28.46	0.05	-5	-152	81.45		44.35	0.06	
6	38	-620	23.96	0.06	24	-509	29.19	0.05	-7	-183	81.19		44.78	0.06	
7	44	-689	25.16	0.06	31	-568	30.52	0.05	-6	-212	81.76		45.81	0.06	
8	51	-749	26.45	0.07	35	-632	31.34	0.06	-8	-241	82.20		46.66	0.07	
9	59	-814	27.38	0.07	43	-686	32.49	0.06	-10	-266	83.78		47.88	0.07	
10	65	-879	28.17	0.07	47	-743	33.33	0.06	-8	-294	84.22		48.57	0.07	
Cycle 1															
10	67	-854	29.00	0.08	54	-702	35.27	0.08	-8	-288	85.98		50.08	0.08	
9	60	-794	28.07	0.08	47	-651	34.23	0.07	-11	-264	84.42		48.91	0.08	
8	56	-744	26.63	0.08	39	-611	32.42	0.06	-15	-240	82.54		47.20	0.07	
7	45	-696	24.90	0.06	32	-553	31.34	0.06	-14	-216	80.25		45.50	0.06	
6	38	-632	23.51	0.06	26	-498	29.83	0.05	-14	-188	79.03		44.12	0.06	
5	31	-558	22.19	0.06	19	-444	27.88	0.04	-11	-161	76.90		42.32	0.05	
4	23	-470	21.07	0.05	14	-371	26.70	0.04	-10	-131	75.61		41.13	0.05	
3	18	-374	19.86	0.05	9	-294	25.27	0.03	-9	-98	75.80		40.31	0.04	
2	12	-256	19.35	0.05	5	-203	24.40	0.02	-5	-63	78.61		40.79	0.04	
1	6	-127	19.50	0.05	1	-102	24.28	0.01	-3	-31	79.88		41.22	0.03	

Table C.3. Results of the second cycle of the biaxial test on the inside of Specimen 208-019-OC1-14.55

P (MPa)	e_1 $\times 10^6$	e_3 $\times 10^6$	E (GPa)	ν	e_5 $\times 10^6$	e_7 $\times 10^6$	E (GPa)	ν	e_9 $\times 10^6$	e_{11} $\times 10^6$	E (GPa)	ν	E_{av} (GPa)	ν_{av}
1	-3	-104	23.81		7	-84	29.48	0.08	3	-27	91.71		48.33	
2	6	-214	23.14	0.03	10	-172	28.79	0.06	0	-57	86.88		46.27	0.05
3	10	-325	22.86	0.03	12	-261	28.46	0.05	0	-93	79.88		43.73	0.04
4	17	-429	23.09	0.04	16	-340	29.13	0.05	5	-121	81.86		44.69	0.05
5	24	-522	23.72	0.05	23	-413	29.98	0.06	6	-149	83.09		45.60	0.06
6	32	-604	24.60	0.05	28	-479	31.02	0.06	4	-180	82.54		46.05	0.06
7	39	-670	25.87	0.06	33	-542	31.98	0.06	6	-207	83.74		47.20	0.06
8	44	-742	26.70	0.06	38	-599	33.07	0.06	1	-237	83.58		47.78	0.06
9	51	-803	27.75	0.06	44	-652	34.18	0.07	8	-264	84.42		48.78	0.07
10	60	-864	28.66	0.07	53	-705	35.12	0.08	8	-288	85.98		49.92	0.08
Cycle 2														
10	67	-863	28.69	0.08	51	-697	35.53	0.07	-8	-290	85.39		49.87	0.08
9	58	-812	27.45	0.07	43	-651	34.23	0.07	-10	-265	84.10		48.59	0.07
8	52	-759	26.10	0.07	36	-608	32.58	0.06	-10	-243	81.52		46.73	0.07
7	44	-698	24.83	0.06	27	-554	31.29	0.05	-10	-218	79.51		45.21	0.06
6	38	-631	23.55	0.06	22	-493	30.14	0.04	-6	-189	78.61		44.10	0.05
5	29	-554	22.35	0.05	17	-436	28.40	0.04	-25	-163	75.96		42.24	0.05
4	22	-460	21.53	0.05	8	-364	27.21	0.02	12	-131	75.61		41.45	0.04
3	20	-368	20.19	0.05	6	-285	26.07	0.02	22	-100	74.29		40.18	0.04
2	9	-252	19.65	0.04	0	-199	24.86	0.00	32	-68	72.83		39.11	0.02
1	5	-131	18.90	0.04	-1	-100	24.76	0.00	-10	-32	77.38		40.35	0.02

Table C.4. Results of the third cycle of the biaxial test on the inside of Specimen 208-019-OC1-14.55

P (MPa)	e_1 $\times 10^6$	e_3 $\times 10^6$	E (GPa)	ν	e_5 $\times 10^6$	e_7 $\times 10^6$	E (GPa)	ν	e_9 $\times 10^6$	e_{11} $\times 10^6$	E (GPa)	ν	E_{av} (GPa)	ν_{av}	
1	6	-104	23.81	0.06	4	-83	29.83	0.05	2	-28	88.44		47.36	0.06	
2	10	-221	22.41	0.05	6	-171	28.96	0.04	0	-56	88.44		46.60	0.05	
3	19	-331	22.44	0.06	12	-257	28.90	0.05	0	-86	86.38		45.91	0.06	
4	26	-430	23.03	0.06	15	-335	29.57	0.04	0	-117	84.66		45.75	0.05	
5	32	-520	23.81	0.06	22	-412	30.05	0.05	0	-151	81.99		45.28	0.06	
6	39	-609	24.40	0.06	27	-480	30.95	0.06	3	-180	82.54		45.96	0.06	
7	48	-677	25.60	0.07	33	-541	32.04	0.06	4	-208	83.33		46.99	0.07	
8	56	-744	26.63	0.08	38	-601	32.96	0.06	2	-233	85.02		48.20	0.07	
9	61	-806	27.65	0.08	43	-652	34.18	0.07	0	-261	85.39		49.07	0.08	
10	65	-864	28.66	0.08	51	-705	35.12	0.07	-5	-287	86.28		50.02	0.08	
Cycle 3															
10	64	-862	28.73	0.07	52	-701	35.32	0.07	-7	-293	84.51		49.52	0.07	
9	57	-812	27.45	0.07	45	-654	34.08	0.07	-2	-266	83.78		48.44	0.07	
8	48	-761	26.03	0.06	37	-608	32.58	0.06	-2	-245	80.86		46.49	0.06	
7	41	-697	24.87	0.06	34	-558	31.06	0.06	-2	-218	79.51		45.15	0.06	
6	36	-637	23.32	0.06	26	-501	29.65	0.05	-2	-190	78.20		43.72	0.06	
5	31	-558	22.19	0.06	20	-439	28.20	0.05	-2	-162	76.43		42.27	0.06	
4	20	-469	21.12	0.04	12	-369	26.84	0.03	-2	-131	75.61		41.19	0.04	
3	13	-378	19.65	0.03	9	-293	25.35	0.03	-4	-102	72.83		39.28	0.03	
2	7	-262	18.90	0.03	5	-205	24.16	0.02	-2	-68	72.83		38.63	0.03	
1	3	-131	18.90	0.02	2	-106	23.36	0.02	2	-34	72.83		38.36	0.02	

Table C.5. Results of the biaxial test with axial load on the outside of Specimen 208-019-OC1-14.55

loading	cycle 1		cycle 2		cycle 3		unloading	cycle 1		cycle 2		cycle 3	
	P (MPa)	$e_l \times 10^6$	E (GPa)	$e_l \times 10^6$	E (GPa)	$e_l \times 10^6$	E (GPa)	P (MPa)	$e_l \times 10^6$	E (GPa)	$e_l \times 10^6$	E (GPa)	$e_l \times 10^6$
2	-13	190.48	-22	112.55	-23	107.66	36	-451	98.83	-454	98.17	-453	98.39
4	-49	101.07	-62	79.88	-65	76.19	34	-445	94.60	-448	93.96	-447	94.17
6	-91	81.63	-106	70.08	-109	68.18	32	-436	90.87	-438	90.45	-437	90.66
8	-135	73.37	-150	66.03	-152	65.16	30	-425	87.39	-426	87.19	-425	87.39
10	-175	70.75	-189	65.51	-191	64.82	28	-410	84.55	-414	83.74	-414	83.74
12	-212	70.08	-224	66.33	-226	65.74	26	-400	80.48	-402	80.08	-401	80.28
14	-244	71.04	-255	67.97	-257	67.44	24	-388	76.58	-389	76.39	-387	76.78
16	-272	72.83	-283	70.00	-283	70.00	22	-373	73.02	-376	72.44	-374	72.83
18	-294	75.80	-308	72.36	-308	72.36	20	-357	69.36	-359	68.97	-358	69.17
20	-316	78.36	-330	75.04	-330	75.04	18	-339	65.74	-342	65.16	-341	65.35
22	-335	81.31	-349	78.05	-349	78.05	16	-320	61.90	-325	60.95	-322	61.52
24	-353	84.18	-365	81.41	-363	81.86	14	-298	58.17	-302	57.40	-299	57.97
26	-368	87.47	-380	84.71	-379	84.94	12	-273	54.42	-274	54.22	-274	54.22
28	-381	90.99	-395	87.76	-392	88.44	10	-241	51.37	-243	50.95	-243	50.95
30	-393	94.51	-406	91.48	-403	92.17	8	-204	48.55	-205	48.32	-206	48.08
32	-405	97.82	-418	94.78	-415	95.47	6	-163	45.57	-163	45.57	-164	45.30
34	-414	101.68	-429	98.12	-426	98.81	4	-111	44.62	-113	43.83	-112	44.22
36	-422	105.62	-437	101.99	-436	102.23	2	-56	44.22	-58	42.69	-58	42.69

Table C.6. Results of the first cycle of the biaxial test with axial load on the inside of Specimen 208-019-OC1-14.55

P (MPa)	e_1 $\times 10^6$	E (GPa)	e_5 $\times 10^6$	E (GPa)	e_9 $\times 10^6$	E (GPa)	E_{av} (GPa)	P (MPa)	e_1 $\times 10^6$	E (GPa)	e_5 $\times 10^6$	E (GPa)	e_9 $\times 10^6$	E (GPa)	E_{av} (GPa)
2	-47	52.68	-54	45.86	-40		49.27	36	-448	99.49	-480	92.86	-740		96.18
4	-85	58.26	-97	51.06	-100		54.66	34	-442	95.24	-473	89.00	-742		92.12
6	-122	60.89	-139	53.44	-170		57.17	32	-429	92.35	-453	87.46	-710		89.91
8	-158	62.69	-176	56.28	-230		59.49	30	-417	89.07	-447	83.09	-680		86.08
10	-190	65.16	-213	58.13	-290		61.65	28	-402	86.24	-433	80.06	-660		83.15
12	-225	66.03	-245	60.64	-340		63.34	26	-387	83.18	-419	76.83	-620		80.01
14	-252	68.78	-276	62.80	-390		65.79	24	-372	79.88	-403	73.73	-600		76.81
16	-280	70.75	-304	65.16	-440		67.96	22	-355	76.73	-387	70.38	-570		73.56
18	-305	73.07	-332	67.13	-480		70.10	20	-340	72.83	-370	66.92	-540		69.88
20	-330	75.04	-354	69.95	-520		72.50	18	-318	70.08	-351	63.49	-510		66.79
22	-352	77.38	-379	71.87	-560		74.63	16	-300	66.03	-330	60.03	-470		63.03
24	-372	79.88	-401	74.10	-590		76.99	14	-279	62.13	-305	56.83	-430		59.48
26	-392	82.12	-422	76.28	-630		79.20	12	-256	58.04	-284	52.31	-390		55.18
28	-410	84.55	-440	78.79	-660		81.67	10	-228	54.30	-254	48.74	-340		51.52
30	-427	86.99	-456	81.45	-690		84.22	8	-199	49.77	-222	44.62	-290		47.20
32	-444	89.23	-474	83.58	-720		86.41	6	-162	45.86	-183	40.59	-230		43.23
34	-462	91.12	-493	85.39	-740		88.26	4	-124	39.94	-139	35.63	-160		37.79
36	-478	93.25	-509	87.57	-770		90.41	2	-77	32.16	-86	28.79	-80		30.48

Table C.7. Results of the second cycle of the biaxial test with axial load on the inside of Specimen 208-019-OC1-14.55

P (MPa)	e_1 $\times 10^6$	E (GPa)	e_5 $\times 10^6$	E (GPa)	e_9 $\times 10^6$	E (GPa)	E_{av} (GPa)	P (MPa)	e_1 $\times 10^6$	E (GPa)	e_5 $\times 10^6$	E (GPa)	e_9 $\times 10^6$	E (GPa)	E (GPa)	E_{av} (GPa)
2	-38	65.16	-50	49.52	-50		57.34	36	-435	102.46	-471	94.63	-730			98.55
4	-75	66.03	-94	52.68	-110		59.36	34	-431	97.67	-464	90.72	-720			94.20
6	-113	65.74	-133	55.85	-170		60.80	32	-416	95.24	-451	87.85	-690			91.55
8	-148	66.92	-169	58.61	-220		62.77	30	-401	92.63	-437	84.99	-670			88.81
10	-179	69.17	-202	61.29	-280		65.23	28	-388	89.35	-424	81.76	-650			85.55
12	-206	72.12	-233	63.76	-330		67.94	26	-374	86.07	-403	79.88	-620			82.98
14	-237	73.14	-263	65.91	-380		69.53	24	-359	82.77	-390	76.19	-590			79.48
16	-262	75.61	-290	68.31	-420		71.96	22	-343	79.41	-375	72.63	-560			76.02
18	-286	77.92	-313	71.20	-460		74.56	20	-325	76.19	-359	68.97	-530			72.58
20	-309	80.14	-336	73.70	-500		76.92	18	-309	72.12	-340	65.55	-500			68.84
22	-329	82.79	-358	76.08	-540		79.44	16	-289	68.54	-319	62.10	-460			65.32
24	-349	85.14	-379	78.40	-570		81.77	14	-265	65.41	-293	59.16	-420			62.29
26	-366	87.95	-397	81.08	-600		84.52	12	-240	61.90	-271	54.82	-380			58.36
28	-385	90.04	-413	83.94	-630		86.99	10	-212	58.40	-240	51.59	-340			55.00
30	-400	92.86	-431	86.18	-650		89.52	8	-182	54.42	-205	48.32	-280			51.37
32	-418	94.78	-450	88.04	-680		91.41	6	-147	50.53	-168	44.22	-220			47.38
34	-433	97.22	-464	90.72	-700		93.97	4	-105	47.17	-124	39.94	-150			43.56
36	-448	99.49	-481	92.66	-730		96.08	2	-59	41.97	-70	35.37	-70			38.67

Table C.8. Results of the third cycle of the biaxial test with axial load on the inside of Specimen 208-019-OC1-14.55

P (MPa)	e_1 $\times 10^6$	E (GPa)	e_5 $\times 10^6$	E (GPa)	e_9 $\times 10^6$	E (GPa)	E_{av} (GPa)	P (MPa)	e_1 $\times 10^6$	E (GPa)	e_5 $\times 10^6$	E (GPa)	e_9 $\times 10^6$	E (GPa)	E_{av} (GPa)
2	-28	88.44	-33	75.04	-40		81.74	36	-440	101.30	-475	93.83	-730		97.57
4	-67	73.92	-81	61.14	-100		67.53	34	-436	96.55	-468	89.95	-710		93.25
6	-103	72.12	-121	61.39	-160		66.76	32	-420	94.33	-453	87.46	-690		90.90
8	-138	71.77	-157	63.09	-220		67.43	30	-409	90.81	-442	84.03	-670		87.42
10	-170	72.83	-193	64.15	-280		68.49	28	-394	87.99	-427	81.19	-640		84.59
12	-201	73.92	-224	66.33	-330		70.13	26	-379	84.94	-413	77.94	-610		81.44
14	-229	75.69	-255	67.97	-380		71.83	24	-362	82.08	-398	74.66	-590		78.37
16	-256	77.38	-283	70.00	-420		73.69	22	-348	78.27	-382	71.30	-560		74.79
18	-279	79.88	-304	73.31	-460		76.60	20	-331	74.81	-364	68.03	-530		71.42
20	-301	82.27	-328	75.49	-500		78.88	18	-312	71.43	-345	64.60	-500		68.02
22	-323	84.33	-350	77.82	-540		81.08	16	-291	68.07	-325	60.95	-460		64.51
24	-342	86.88	-370	80.31	-570		83.60	14	-270	64.20	-302	57.40	-420		60.80
26	-362	88.92	-389	82.75	-600		85.84	12	-248	59.91	-275	54.03	-380		56.97
28	-376	92.20	-406	85.39	-630		88.80	10	-220	56.28	-248	49.92	-330		53.10
30	-394	94.27	-424	87.60	-660		90.94	8	-190	52.13	-217	45.64	-280		48.89
32	-410	96.63	-438	90.45	-680		93.54	6	-153	48.55	-180	41.27	-220		44.91
34	-424	99.28	-452	93.13	-710		96.21	4	-111	44.62	-133	37.24	-150		40.93
36	-439	101.53	-468	95.24	-730		98.39	2	-65	38.10	-79	31.34	-70		34.72

Appendix D

Specimen 208-019-OC1-15.50

Table D.1. Results of the biaxial test on the outside of Specimen 208-019-OC1-15.50

P (MPa)	cycle 1				cycle 2				cycle 3			
	e_t $\times 10^6$	e_l $\times 10^6$	E (GPa)	ν	e_t $\times 10^6$	e_l $\times 10^6$	E (GPa)	ν	e_t $\times 10^6$	e_l $\times 10^6$	E (GPa)	ν
1	-56	8	26.28	0.14	-48	9	30.66	0.19	-51	11	28.85	0.22
2	-111	13	26.51	0.12	-104	13	28.30	0.13	-106	18	27.76	0.17
3	-169	23	26.12	0.14	-159	24	27.76	0.15	-162	26	27.25	0.16
4	-219	29	26.88	0.13	-211	27	27.90	0.13	-213	34	27.63	0.16
5	-271	38	27.15	0.14	-259	39	28.41	0.15	-259	39	28.41	0.15
6	-316	44	27.94	0.14	-301	43	29.33	0.14	-302	50	29.24	0.17
7	-360	54	28.61	0.15	-340	54	30.30	0.16	-340	55	30.30	0.16
8	-397	61	29.65	0.15	-375	59	31.39	0.16	-375	66	31.39	0.18
9	-434	69	30.52	0.16	-407	71	32.54	0.17	-407	71	32.54	0.17
10	-473	75	31.11	0.16	-438	75	33.60	0.17	-437	82	33.67	0.19
10	-437	69	33.67	0.16	-435	80	33.83	0.18	-435	72	33.83	0.17
9	-413	63	32.07	0.15	-411	77	32.22	0.19	-412	70	32.15	0.17
8	-383	55	30.74	0.14	-384	66	30.66	0.17	-385	60	30.58	0.16
7	-355	48	29.02	0.14	-355	62	29.02	0.17	-356	57	28.93	0.16
6	-320	39	27.59	0.12	-322	53	27.42	0.16	-322	46	27.42	0.14
5	-285	33	25.82	0.12	-284	44	25.91	0.15	-285	42	25.82	0.15
4	-240	25	24.53	0.10	-241	35	24.42	0.15	-242	33	24.32	0.14
3	-191	20	23.11	0.10	-190	27	23.23	0.14	-191	27	23.11	0.14
2	-132	11	22.30	0.08	-131	15	22.47	0.11	-132	14	22.30	0.11
1	-69	6	21.33	0.09	-66	9	22.30	0.14	-68	9	21.64	0.13

Table D.2. Results of the first cycle of the biaxial test on the inside of Specimen 208-019-OC1-15.50

P (MPa)	e_1 $\times 10^6$	e_3 $\times 10^6$	E (GPa)	ν	e_5 $\times 10^6$	e_7 $\times 10^6$	E (GPa)	ν	e_9 $\times 10^6$	e_{11} $\times 10^6$	E (GPa)	ν	E_{av} (GPa)	ν_{av}
1	8	-62	39.86	0.13	6	-73	33.86	0.08	11	-55	44.94	0.20	39.55	0.14
2	16	-114	43.36	0.14	9	-160	30.89	0.06	13	-117	42.25	0.11	38.83	0.10
3	22	-179	41.42	0.12	16	-240	30.89	0.07	19	-168	44.13	0.11	38.81	0.10
4	28	-244	40.52	0.11	22	-321	30.80	0.07	27	-213	46.41	0.13	39.24	0.10
5	34	-306	40.38	0.11	28	-396	31.21	0.07	31	-261	47.35	0.12	39.65	0.10
6	42	-365	40.63	0.12	36	-469	31.62	0.08	38	-293	50.61	0.13	40.95	0.11
7	50	-421	41.09	0.12	40	-537	31.22	0.07	45	-335	51.64	0.13	41.32	0.11
8	56	-474	41.71	0.12	46	-602	32.84	0.08	51	-363	54.47	0.14	43.01	0.11
9	65	-529	42.05	0.12	54	-662	33.60	0.08	58	-391	56.89	0.15	44.18	0.12
10	76	-581	42.54	0.13	60	-722	34.23	0.08	64	-418	59.13	0.15	45.30	0.12
Cycle 1														
10	72	-554	44.61	0.13	58	-677	36.51	0.09	61	-385	64.20	0.16	48.44	0.13
9	61	-505	44.05	0.12	50	-629	35.36	0.08	54	-364	61.11	0.15	46.84	0.12
8	50	-464	42.61	0.11	47	-585	33.80	0.08	47	-346	57.15	0.14	44.52	0.11
7	43	-425	40.71	0.10	39	-531	32.58	0.07	40	-323	53.56	0.12	42.28	0.10
6	35	-376	39.44	0.09	33	-478	31.02	0.07	33	-299	49.60	0.11	40.02	0.09
5	28	-325	38.02	0.09	26	-416	29.71	0.06	25	-271	45.60	0.09	37.78	0.08
4	24	-266	37.17	0.09	22	-340	29.08	0.06	19	-237	41.71	0.08	35.99	0.08
3	14	-209	35.48	0.07	17	-272	27.26	0.06	14	-195	38.02	0.07	33.59	0.07
2	11	-144	34.33	0.08	7	-192	25.75	0.04	7	-145	34.09	0.05	31.39	0.06
1	3	-73	33.86	0.04	3	-101	24.47	0.03	3	-78	31.69	0.04	30.01	0.04

Table D.3. Results of the second cycle of the biaxial test on the inside of Specimen 208-019-OC1-15.50

P (MPa)	e_1 $\times 10^6$	e_3 $\times 10^6$	E (GPa)	ν	e_5 $\times 10^6$	e_7 $\times 10^6$	E (GPa)	ν	e_9 $\times 10^6$	e_{11} $\times 10^6$	E (GPa)	ν	E_{av} (GPa)	ν_{av}	
1	7	-59	41.89	0.12	3	-91	27.16	0.03	3	-103	24.00	0.03	31.02	0.06	
2	14	-117	42.25	0.12	9	-166	29.78	0.05	8	-212	23.32	0.04	31.78	0.07	
3	22	-177	41.89	0.12	13	-241	30.77	0.05	13	-320	23.17	0.04	31.94	0.07	
4	28	-239	41.36	0.12	21	-326	30.33	0.06	20	-416	23.76	0.05	31.82	0.08	
5	35	-296	41.75	0.12	25	-396	31.21	0.06	29	-502	24.62	0.06	32.53	0.08	
6	44	-353	42.01	0.12	30	-469	31.62	0.06	33	-577	25.70	0.06	33.11	0.08	
7	48	-408	42.40	0.12	36	-535	32.34	0.07	38	-649	26.66	0.06	33.80	0.08	
8	52	-459	43.08	0.11	41	-594	33.29	0.07	44	-710	27.85	0.06	34.74	0.08	
9	59	-509	43.70	0.12	48	-648	34.33	0.07	51	-767	29.00	0.07	35.68	0.09	
10	65	-558	44.29	0.12	52	-700	35.31	0.07	56	-822	30.07	0.07	36.56	0.09	
Cycle 2															
10	67	-553	44.69	0.12	56	-674	36.67	0.08	60	-814	30.36	0.07	37.24	0.09	
9	59	-509	43.70	0.12	50	-632	35.20	0.08	54	-768	28.96	0.07	35.95	0.09	
8	52	-469	42.16	0.11	45	-585	33.80	0.08	46	-718	27.54	0.06	34.50	0.08	
7	46	-420	41.19	0.11	40	-527	32.83	0.08	41	-665	26.02	0.06	33.35	0.08	
6	40	-372	39.86	0.11	32	-475	31.22	0.07	31	-606	24.47	0.05	31.85	0.08	
5	34	-320	38.62	0.11	27	-411	30.07	0.07	26	-538	22.97	0.05	30.55	0.08	
4	28	-264	37.45	0.11	20	-342	28.91	0.06	18	-460	21.49	0.04	29.28	0.07	
3	17	-204	36.35	0.08	16	-268	27.67	0.06	14	-369	20.09	0.04	28.04	0.06	
2	10	-135	36.62	0.07	7	-179	27.61	0.04	9	-260	19.01	0.03	27.75	0.05	
1	3	-73	33.86	0.04	3	-95	26.02	0.03	2	-133	18.58	0.02	26.15	0.03	

Table D.4. Results of the third cycle of the biaxial test on the inside of Specime 208-019-OC1-15.50

P (MPa)	e_1 $\times 10^6$	e_3 $\times 10^6$	E (GPa)	ν	e_5 $\times 10^6$	e_7 $\times 10^6$	E (GPa)	ν	e_9 $\times 10^6$	e_{11} $\times 10^6$	E (GPa)	ν	E_{av} (GPa)	ν_{av}
1	8	-61	40.52	0.13	4	-76	32.52	0.05	5	-106	23.32	0.05	32.12	0.08
2	17	-117	42.25	0.15	11	-153	32.31	0.07	11	-211	23.43	0.05	32.66	0.09
3	24	-179	41.42	0.13	19	-232	31.96	0.08	17	-323	22.96	0.05	32.11	0.09
4	28	-238	41.54	0.12	24	-307	32.20	0.08	24	-417	23.71	0.06	32.48	0.09
5	37	-296	41.75	0.13	29	-381	32.43	0.08	30	-503	24.57	0.06	32.92	0.09
6	41	-352	42.13	0.12	35	-449	33.03	0.08	37	-572	25.93	0.06	33.70	0.09
7	49	-406	42.61	0.12	40	-511	33.86	0.08	41	-642	26.95	0.06	34.47	0.09
8	55	-457	43.27	0.12	45	-573	34.51	0.08	48	-707	27.97	0.07	35.25	0.09
9	66	-504	44.13	0.13	52	-628	35.42	0.08	54	-762	29.19	0.07	36.25	0.09
10	72	-552	44.77	0.13	58	-682	36.24	0.09	61	-814	30.36	0.07	37.12	0.10
Cycle 3														
10	68	-554	44.61	0.12	59	-678	36.45	0.09	62	-815	30.33	0.08	37.13	0.10
9	58	-513	43.36	0.11	52	-631	35.25	0.08	54	-765	29.08	0.07	35.90	0.09
8	56	-470	42.07	0.12	45	-585	33.80	0.08	45	-721	27.42	0.06	34.43	0.09
7	44	-423	40.90	0.10	40	-530	32.64	0.08	39	-668	25.90	0.06	33.15	0.08
6	41	-370	40.08	0.11	35	-474	31.29	0.07	34	-609	24.35	0.06	31.91	0.08
5	28	-319	38.74	0.09	28	-411	30.07	0.07	25	-541	22.84	0.05	30.55	0.07
4	24	-261	37.88	0.09	21	-342	28.91	0.06	18	-465	21.26	0.04	29.35	0.06
3	17	-202	36.71	0.08	15	-267	27.77	0.06	13	-373	19.88	0.03	28.12	0.06
2	9	-134	36.89	0.07	9	-180	27.46	0.05	8	-261	18.94	0.03	27.76	0.05
1	5	-72	34.33	0.07	3	-91	27.16	0.03	4	-136	18.17	0.03	26.55	0.04

Table D.5. Results of the biaxial test with axial load on the outside of Specimen 208-019-OC1-15.50

loading	cycle 1		cycle 2		cycle 3		unloading	cycle 1		cycle 2		cycle 3	
	P (MPa)	e_l $\times 10^6$	E (GPa)	e_l $\times 10^6$	E (GPa)	e_l $\times 10^6$	E (GPa)	P (MPa)	e_l $\times 10^6$	E (GPa)	e_l $\times 10^6$	E (GPa)	e_l $\times 10^6$
2	-24	102.98	-32	77.24	-31	79.73	36	-441	100.88	-448	99.30	-444	100.20
4	-63	78.46	-68	72.69	-69	71.64	34	-439	95.71	-445	94.42	-438	95.93
6	-104	71.29	-106	69.95	-110	67.41	32	-429	92.18	-436	90.70	-428	92.39
8	-141	70.11	-143	69.13	-150	65.91	30	-416	89.12	-421	88.06	-416	89.12
10	-178	69.43	-180	68.65	-186	66.44	28	-402	86.07	-409	84.60	-405	85.44
12	-214	69.30	-213	69.62	-218	68.02	26	-390	82.38	-394	81.55	-391	82.17
14	-248	69.76	-243	71.20	-245	70.62	24	-376	78.88	-380	78.05	-376	78.88
16	-272	72.69	-271	72.96	-274	72.16	22	-362	75.10	-365	74.48	-362	75.10
18	-299	74.39	-299	74.39	-296	75.15	20	-344	71.85	-351	70.41	-346	71.43
20	-322	76.76	-322	76.76	-320	77.24	18	-329	67.61	-332	67.00	-328	67.82
22	-346	78.57	-342	79.49	-339	80.20	16	-309	63.99	-313	63.17	-308	64.20
24	-365	81.26	-364	81.48	-357	83.08	14	-287	60.28	-290	59.66	-288	60.07
26	-383	83.89	-379	84.78	-374	85.91	12	-262	56.60	-265	55.96	-261	56.82
28	-401	86.29	-400	86.50	-389	88.95	10	-231	53.60	-237	52.14	-232	53.27
30	-416	89.12	-410	90.42	-402	92.22	8	-199	49.68	-203	48.72	-198	49.93
32	-432	91.54	-426	92.83	-418	94.60	6	-159	46.63	-164	45.21	-158	46.93
34	-445	94.42	-440	95.49	-430	97.71	4	-111	44.53	-118	41.89	-111	44.53
36	-460	96.71	-455	97.78	-444	100.20	2	-59	41.89	-67	36.89	-60	41.19

Table D.6. Results of the first cycle of the biaxial test with axial load on the inside of Specimen 208-019-OC1-15.50

P (MPa)	e_1 $\times 10^6$	E (GPa)	e_5 $\times 10^6$	E (GPa)	e_9 $\times 10^6$	E (GPa)	E_{av} (GPa)	P (MPa)	e_1 $\times 10^6$	E (GPa)	e_5 $\times 10^6$	E (GPa)	e_9 $\times 10^6$	E (GPa)	E_{av} (GPa)
2	-35	70.62	-19	130.08	-10	247.15	149.28	36	-506	87.92	-467	95.26	-380	117.07	100.08
4	-90	54.92	-63	78.46	-28	176.54	103.31	34	-504	83.37	-462	90.94	-378	111.15	95.15
6	-136	54.52	-104	71.29	-56	132.40	86.07	32	-491	80.54	-447	88.47	-365	108.34	92.45
8	-180	54.92	-143	69.13	-89	111.08	78.38	30	-478	77.56	-433	85.62	-353	105.02	89.40
10	-219	56.43	-180	68.65	-119	103.85	76.31	28	-465	74.41	-416	83.18	-343	100.88	86.16
12	-258	57.48	-213	69.62	-155	95.67	74.26	26	-450	71.40	-394	81.55	-329	97.66	83.54
14	-291	59.45	-242	71.49	-183	94.54	75.16	24	-433	68.50	-381	77.84	-315	94.15	80.16
16	-324	61.03	-274	72.16	-216	91.54	74.91	22	-418	65.04	-364	74.69	-299	90.93	76.89
18	-354	62.84	-304	73.17	-244	91.16	75.72	20	-397	62.26	-343	72.06	-284	87.03	73.78
20	-381	64.87	-329	75.12	-268	92.22	77.40	18	-378	58.85	-323	68.87	-268	83.00	70.24
22	-405	67.13	-353	77.02	-288	94.40	79.52	16	-355	55.70	-301	65.69	-250	79.09	66.83
24	-431	68.81	-375	79.09	-304	97.56	81.82	14	-330	52.43	-277	62.46	-229	75.55	63.48
26	-452	71.08	-399	80.53	-327	98.26	83.29	12	-302	49.10	-251	59.08	-206	71.99	60.06
28	-474	73.00	-420	82.38	-342	101.17	85.52	10	-268	46.11	-220	56.17	-181	68.27	56.85
30	-490	75.66	-438	84.64	-358	103.56	87.95	8	-228	43.36	-184	53.73	-150	65.91	54.33
32	-508	77.84	-455	86.91	-376	105.17	89.97	6	-185	40.08	-144	51.49	-113	65.62	52.40
34	-525	80.03	-474	88.64	-390	107.73	92.13	4	-124	39.86	-102	48.46	-74	66.80	51.71
36	-542	82.08	-492	90.42	-405	109.85	94.12	2	-76	32.52	-52	47.53	-33	74.90	51.65

Table D.7. Results of the second cycle of the biaxial test with axial load on the inside of Specimen 208-019-OC1-15.50

P (MPa)	e_1 $\times 10^6$	E (GPa)	e_5 $\times 10^6$	E (GPa)	e_9 $\times 10^6$	E (GPa)	E_{av} (GPa)	P (MPa)	e_1 $\times 10^6$	E (GPa)	e_5 $\times 10^6$	E (GPa)	e_9 $\times 10^6$	E (GPa)	E_{av} (GPa)
2	-40	61.79	-20	123.58	-16	154.47	113.28	36	-507	87.75	-471	94.45	-386	115.25	99.15
4	-91	54.32	-66	74.90	-39	126.75	85.32	34	-505	83.20	-462	90.94	-382	109.99	94.71
6	-135	54.92	-105	70.62	-70	105.92	77.15	32	-495	79.89	-450	87.88	-371	106.59	91.45
8	-175	56.49	-138	71.64	-103	95.98	74.70	30	-483	76.76	-435	85.23	-357	103.85	88.61
10	-213	58.02	-177	69.82	-135	91.54	73.13	28	-466	74.25	-419	82.58	-345	100.29	85.71
12	-249	59.56	-208	71.29	-163	90.98	73.94	26	-448	71.72	-401	80.12	-331	97.07	82.97
14	-284	60.92	-241	71.79	-192	90.11	74.27	24	-432	68.65	-384	77.24	-318	93.27	79.72
16	-313	63.17	-265	74.61	-210	94.15	77.31	22	-418	65.04	-366	74.28	-302	90.02	76.45
18	-342	65.04	-295	75.40	-239	93.07	77.84	20	-400	61.79	-347	71.23	-286	86.42	73.15
20	-367	67.34	-319	77.48	-262	94.33	79.72	18	-377	59.00	-326	68.23	-270	82.38	69.87
22	-390	69.71	-340	79.96	-282	96.41	82.03	16	-353	56.01	-304	65.04	-252	78.46	66.50
24	-411	72.16	-364	81.48	-301	98.53	84.06	14	-330	52.43	-277	62.46	-231	74.90	63.26
26	-435	73.86	-385	83.45	-318	101.04	86.12	12	-300	49.43	-251	59.08	-209	70.95	59.82
28	-451	76.72	-404	85.65	-335	103.29	88.55	10	-269	45.94	-221	55.92	-182	67.90	56.59
30	-468	79.22	-421	88.06	-348	106.53	91.27	8	-231	42.80	-188	52.59	-152	65.04	53.48
32	-486	81.37	-437	90.49	-363	108.94	93.60	6	-186	39.86	-149	49.76	-117	63.37	51.00
34	-500	84.03	-456	92.14	-379	110.86	95.68	4	-136	36.35	-104	47.53	-75	65.91	49.93
36	-516	86.22	-473	94.05	-392	113.49	97.92	2	-74	33.40	-55	44.94	-35	70.62	49.65

Table D.8. Results of the third cycle of the biaxial test with axial load on the inside of Specimen 208-019-OC1-15.50

P (MPa)	e_1 $\times 10^6$	E (GPa)	e_5 $\times 10^6$	E (GPa)	e_9 $\times 10^6$	E (GPa)	E_{av} (GPa)	P (MPa)	e_1 $\times 10^6$	E (GPa)	e_5 $\times 10^6$	E (GPa)	e_9 $\times 10^6$	E (GPa)	E_{av} (GPa)
2	-37	66.80	-24	102.98	-21	117.69	95.82	36	-501	88.80	-463	96.09	-403	110.39	98.43
4	-83	59.56	-61	81.03	-54	91.54	77.38	34	-496	84.71	-455	92.34	-401	104.78	93.94
6	-128	57.93	-104	71.29	-82	90.42	73.21	32	-483	81.87	-441	89.67	-386	102.45	91.33
8	-167	59.20	-140	70.62	-124	79.73	69.85	30	-471	78.71	-425	87.23	-376	98.60	88.18
10	-206	59.99	-172	71.85	-155	79.73	70.52	28	-457	75.71	-411	84.19	-363	95.32	85.07
12	-241	61.53	-204	72.69	-184	80.59	71.60	26	-442	72.69	-394	81.55	-350	91.80	82.01
14	-275	62.91	-236	73.31	-211	81.99	72.74	24	-426	69.62	-376	78.88	-337	88.01	78.84
16	-305	64.83	-263	75.18	-235	84.14	74.72	22	-410	66.31	-359	75.73	-323	84.17	75.40
18	-330	67.41	-289	76.97	-257	86.55	76.98	20	-390	63.37	-340	72.69	-305	81.03	72.36
20	-357	69.23	-311	79.47	-280	88.27	78.99	18	-369	60.28	-318	69.95	-291	76.44	68.89
22	-380	71.54	-336	80.91	-299	90.93	81.13	16	-351	56.33	-297	66.57	-261	75.76	66.22
24	-400	74.15	-356	83.31	-316	93.86	83.77	14	-323	53.56	-270	64.08	-251	68.93	62.19
26	-419	76.68	-377	85.23	-331	97.07	86.33	12	-296	50.10	-247	60.04	-225	65.91	58.68
28	-437	79.18	-394	87.82	-345	100.29	89.10	10	-261	47.35	-216	57.21	-197	62.73	55.76
30	-455	81.48	-412	89.98	-359	103.27	91.58	8	-225	43.94	-182	54.32	-170	58.15	52.14
32	-472	83.78	-432	91.54	-378	104.62	93.31	6	-182	40.74	-143	51.85	-135	54.92	49.17
34	-486	86.45	-447	94.00	-392	107.18	95.88	4	-131	37.73	-101	48.94	-93	53.15	46.61
36	-501	88.80	-463	96.09	-403	110.39	98.43	2	-74	33.40	-53	46.43	-47	52.59	44.21

